

Review

# Critical Review on Interrelationship of Electro-Devices in PV Solar Systems with Their Evolution and Future Prospects for MPPT Applications

Weng-Hooi Tan  and Junita Mohamad-Saleh \* 

School of Electrical & Electronic Engineering, Universiti Sains Malaysia, Nibong Tebal 11430, Penang, Malaysia  
\* Correspondence: jms@usm.my

**Abstract:** A photovoltaic (PV) system is composed of a PV panel, controller and boost converter. This review article presents a critical review, contributing to a better understanding of the interrelationship of all these internal devices in the PV system, their respective layouts, fundamental working principles, and architectural effects. The PV panel is a power-generating device. A controller is an electronic device that controls the circulating circuits in a PV system to collect as much PV output as possible from the solar panel. The boost converter is an intermediate device that regulates the PV output based on the duty cycle provided by the controller. This review article also updates readers on the latest information regarding the technological evolution of these interconnected devices, along with their predicted future scope and challenges. Regarding the research on PV panels, this paper explains in depth the mathematical modeling of PV cells, the evolution of solar cell technology over generations, and their future prospects predicted based on the collected evidence. Then, connection patterns of PV modules are studied to better understand the effect of PV array configuration on photovoltaic performance. For the controller, state-of-the-art maximum power point tracking (MPPT) techniques are reviewed under the classification to reveal near-term trends in MPPT applications. On the other hand, various converter topologies proposed from 2020 to 2022 are reviewed in terms of tested frequency, voltage gain, and peak efficiency to comprehend recent evolution trends and future challenges. All presented information is intended to facilitate and motivate researchers to deepen relevant applications in the future.

**Keywords:** PV panel; controller; DC–DC boost converter; solar cell technology in generations; PV array configurations; MPPT techniques and classification; converter topologies



**Citation:** Tan, W.-H.; Mohamad-Saleh, J. Critical Review on Interrelationship of Electro-Devices in PV Solar Systems with Their Evolution and Future Prospects for MPPT Applications. *Energies* **2023**, *16*, 850. <https://doi.org/10.3390/en16020850>

Academic Editor: Surender Reddy Salkuti

Received: 19 December 2022  
Revised: 3 January 2023  
Accepted: 5 January 2023  
Published: 11 January 2023



**Copyright:** © 2023 by the authors. Licensee MDPI, Basel, Switzerland. This article is an open access article distributed under the terms and conditions of the Creative Commons Attribution (CC BY) license (<https://creativecommons.org/licenses/by/4.0/>).

## 1. Introduction

Global energy provision has evolved into a duty and a commitment to the growth of numerous industrial sectors. For ASEAN's emerging nations to develop their industries, modernize their agriculture, boost trade, and enhance transportation, reliable energy is crucial. However, the official infographic released by the ASEAN Energy Centre 2020 study indicates that certain ASEAN nations still have poor electrification rates. So far, Myanmar only has a 44% electrification rate, while Cambodia only has a 68% electrification rate. According to Silitonga's research, Cambodia has the highest energy costs in the area, depriving the majority of its inhabitants of access to electricity [1]. On the downside, there was an energy deficit of 442.5 MW. Insufficient supply, unstable supply and excessive electricity prices are hallmarks of its energy industry.

To address energy shortages in some ASEAN countries, photovoltaic (PV) systems have gained attention [2]. A PV system is an electrical framework device that produces renewable energy by having PV cells transform solar energy into electricity. It has gained popularity due to favorable low maintenance costs, environmental sustainability, economic viability and long lifespan [3]. Since PV systems have been commercialized in many countries, various studies have been conducted on their future development [4–7]. Suggestions

for improvements and adjustments have been made on a regular basis to increase the capacity of the PV system [8].

A complete PV system consists of three primary devices that work together: a PV panel, controller and boost converter. The PV panel is equivalent to a PV array composed of multiple PV modules in series and parallel, wherein the modules are composed of multiple PV cells in series. Here, PV cells are the smallest compounds responsible for generating PV voltage, current and power to the system [9]. In theory, only PV cells exposed to uniform irradiance and temperature can operate at optimal efficiency [10]. The operating temperature of a PV panel should always be consistent because every PV cell shares the same ambient temperature. Therefore, the only factor that primarily affects power generation should be the irradiance level. Under normal circumstances, a PV module will be fully irradiated ( $1000 \text{ W/m}^2$ ), but sometimes the sunlight will be blocked by obstacles such as clouds, trees, birds, etc., causing some PV cells in the module to be shaded and not illuminated. This is the shading effect, where the PV module receives only a percentile of irradiance from the unshaded surface of PV cells [10]. It goes without saying that all individual modules with the same settings will produce different voltage, current and power outputs at different shading degrees [11]. The higher the irradiance level, the higher the efficiency of the PV system and the higher the PV voltage, current and power generated at the panel terminals.

Different connection patterns of PV modules produce different voltage and current outputs. PV modules are connected in series to double the voltage output and in parallel to double the current output [12,13]. PV systems generally require higher voltage outputs, so series-connected PV modules are favorable. However, in practical applications, PV modules will not be completely connected in series, but will also be mixed in parallel [14]. This is to theoretically reduce the risk of defects. Any wiring fault in the series will terminate the power generation of the entire series array. If only the series connection is used, any wiring failure will terminate the entire power generation process of the PV panel, resulting in chain defects of the entire PV system. On the contrary, any wiring fault inside the parallel connection has little effect on the entire power generation process. Although a row of PV power generation circuits will be terminated, the circuit elements in the other rows can still operate normally without major defects. In this case, only a small amount of current is lost, but the maximum voltage at the terminals remains the same [15].

In practice, fully connected PV modules in a panel sometimes experience varying degrees of shading in respective modules. This is what we call the partial shading phenomenon that occurs in PV panel [16]. The PV panel under partial shading effect will generate multiple power peaks at the power-voltage ( $P$ - $V$ ) characteristic curve [17,18]. The number of power peaks corresponds to the number of PV modules with different shading degrees within the panel. The highest power peak in the  $P$ - $V$  curve denotes the maximum power point (MPP), where the optimal power can be extracted from the PV panel. To reach the MPP and thus maximize the power extraction from the PV panel at any given situation, the controller in a PV system necessitates parameter optimization while referencing the PV panel data and environmental data to obtain a best-tuned duty cycle [19]. Overall, the controller is responsible for optimizing the process of tracking the MPP. The main difficulty lies in the nonlinear nature and environmental reliance of PV power generation [20,21]. For the controller to complete the optimization task, there must be a tracking scheme applied to the controller block. It can be a traditional technique, intelligent approach, or metaheuristic optimization algorithm. All attempts to track MPP using any of the above-classified tracking schemes are referred to as maximum power point tracking (MPPT). We also reasonably refer to these adopted tracking approaches as MPPT techniques.

In effect, the controller sends commands to the boost converter via a pulse width modulation (PWM) signal generated based on the tuned duty cycle to control the switching interval of the transistors in the boost converter, thereby indirectly maximizing the PV power generation in the PV panel. Here, the controller mainly acts as a stabilizer to maintain a constant output power in the PV circuit system. However, it is worth noticing that the

boost converter also acts as a voltage regulator, amplifying the PV voltage drawn from the panel to the user.

From a corollary perspective, for Southeast Asia (SEA) to develop a dependable and consistent energy system, energy efficiency is crucial [22]. In accordance with the energy chapter of the 2025 ASEAN Economic Community (AEC) Blueprint, ASEAN abides by the policy in the 2016–2025 ASEAN Action Plan for Energy Cooperation (APAEC) [23]. It intends to raise the intensity of SEA's renewable energy to the predetermined level of 23%. Thus, improving MPPT techniques through additional research and development may be the best approach to advance renewable energy. It is believed that this will also be the best solution to deal with the energy shortage problem in some SEA countries.

This review article contributes to a better understanding of the mathematical concepts of PV systems. It indeed covers all relevant knowledge, including partial shading effects on the  $P$ - $V$  characteristic curve inside the PV panel, the working procedures of MPPT inside the controller, analytical architecture for voltage regulation and stabilization inside the boost converter, etc. It also updates readers the latest information on technological evolution related to these interconnected devices, primarily reviews of solar cell technology, PV array configurations, state-of-the-art MPPT techniques, and novel converter topologies, along with forecast analysis for their future scope and challenges. All presented information is intended to facilitate and motivate readers or researchers to deepen relevant applications in the future.

Here is an outline of this article: Section 1 introduces this review article, Section 2 explains the conspectus of PV systems, Section 3 studies the PV panel, Section 4 studies the boost converter, Section 5 studies the controller, and Section 6 concludes the review work.

## 2. Conspectus of PV Systems

A growing number of projects have begun large-scale implementation of photovoltaic (PV) solar power to replace non-renewable energy in real-world setups [24]. Photovoltaic systems have emerged as prime candidates for power plants, connected via power lines to distribution systems, transmission systems, substations and end-users [25]. It should be noted that power lines are the medium that carry electricity from one location to another, and the process of transferring electricity over vast-distances between two desired locations is called electrical transmission [26]. The most commonly used type of power line is the overhead line, which can carry huge voltages of 100–800 kV and is mainly used for long distance transmission [27]. Efficient transmission of up to 500 km is possible [28]. In theory, the high voltage capacity minimizes the power loss to resistance. Basically, the amount of power is determined by how much current ( $I$ ) passes through a circuit element, how much voltage ( $V$ ) differs at the nodes, and how much power ( $P$ ) is then lost throughout the process. From a more theoretical point of view, the heat dissipated by current travelling across a power cord/line with internal resistance can cause power loss due to resistance [29,30]. As we expand the analysis, the resulting power loss is the square of the total current drop, and the current drops proportionally with increasing voltage [30]. This claim implies that PV systems require the highest voltage available to deliver the greatest amount of power to users with minimal losses. However, there is a constraint, in that the current begins to discharge at 2000 kV, leading to significant losses [31].

A PV system is an electrical frame device that sustains renewable energy [32]. It consists of three main devices: PV panel, boost converter and controller [33]. Figure 1 displays the complete layout of the PV system, including all internal layouts of the interacted electro-devices. The PV panel is a power-generating device that converts solar energy into electrical energy, at which the output of the PV panel terminals is regulated by the boost converter and supplied to the controller. The controller tunes the duty cycle while referencing the input PV data output from the PV panel to generate the desired controlling signal to the boost converter. The boost converter refers to the controlling signal provided by the controller to regulate the PV data output from the PV panel. For ease of understanding, Figure 2 displays the interrelationship diagram for these electro-devices in

a PV system. The output terminal of the boost converter can be linked to the user device, representing the provision of processed PV power to the user, albeit not directly. The following sections provide an in-depth explanation of each device in terms of background, architecture, concept, and impact.

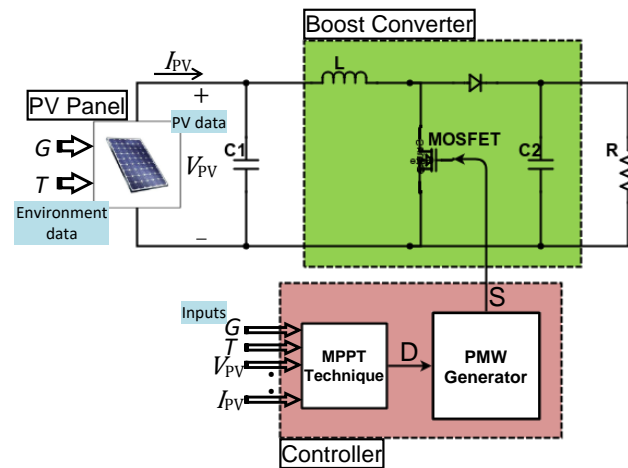


Figure 1. Layout in PV system.

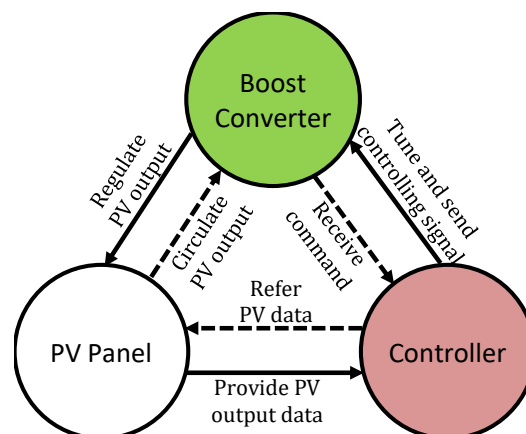


Figure 2. Interrelationship diagram in PV system.

The review sets forth to reveal tendencies in scholarly publications up to the end of December 2022. After in-depth investigation, we collected rough data from journals, conferences, books, editorials, and other sources, with at least a significant number of publications from emerging publishers. The content may include studies from various perspectives such as application, design, modification, evaluation, performance comparison, analysis, discussion, interpretation, etc.; all directly or indirectly contribute to the development of PV-related technologies.

For ease of observation and discussion, this review paper presents the data in different forms such as tables, line charts and pie charts for the following contents. Table 1 records the year-specific publication count by article type, Figure 3 illustrates a line chart plotting publication count by article type over the years, while Figure 4 demonstrates a pie chart with cumulative percentiles distributed by article type.

**Table 1.** Year-specific publication count by article type.

Article Type	Publication Count by Article Type																						Cumulative	
	2000	2001	2002	2003	2004	2005	2006	2007	2008	2009	2010	2011	2012	2013	2014	2015	2016	2017	2018	2019	2020	2021		2022
Research paper	496	515	437	598	643	842	1029	1058	1288	1722	2080	3224	3538	4500	5397	5767	6233	7184	7852	8707	9627	10,402	11,181	94,320
Conference paper	592	100	597	293	215	758	978	427	1010	1558	1952	2388	2701	2789	3193	3370	3847	4119	4779	4873	4593	5147	4332	54,611
Book chapter	195	101	174	161	127	206	209	251	333	599	434	602	709	965	1106	1128	1284	1328	1707	1864	2485	2776	3019	21,763
Review paper	54	58	62	71	90	100	106	127	167	238	262	408	429	465	538	694	825	917	995	1088	1317	1906	3037	13,954
Encyclopaedias	3	34	3	5	9	5	5	22	14	14	5	10	141	99	91	115	111	95	184	199	185	363	256	1968
Editorial	15	7	6	5	3	5	3	6	5	10	12	14	10	21	24	30	21	27	19	24	37	44	51	399
Total	1355	815	1279	1133	1087	1916	2330	1891	2817	4141	4745	6646	7528	8839	10,349	11,104	12,321	13,670	15,536	16,755	18,244	20,638	21,876	187,015

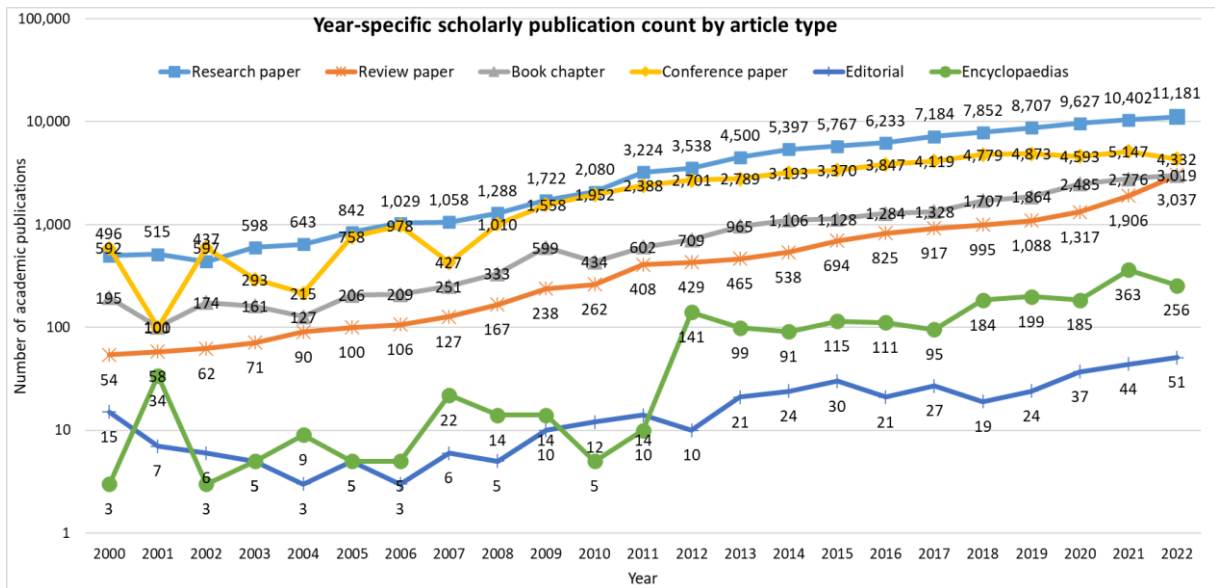


Figure 3. Distribution of publications by article type over the years.

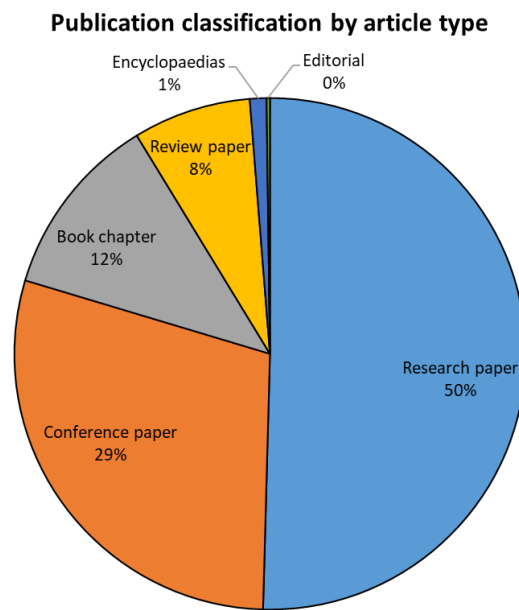


Figure 4. Proportion of publication classification by article type.

The trends in Table 1 and Figure 3 indicate an increasing academic demand for PV-related studies. More than 80% of articles published between 2000 and 2020 were published after 2012, with 2022 seeing the highest number of publications, representing a total increase of 190.6% compared to 2012. Incidentally, the publication count has grown by an average of 11.3% per year over these 10 years. In the decade since 2012, the number of publications across all article types has grown significantly. By the end of 2022, research papers account for the highest proportion of publications (about 50%), followed by conference papers (about 29%), and then book chapters (about 12%), as shown in Figure 4. This reveals that research journals have become the main channel for the dissemination of project outcomes related to the topic of photovoltaics. In fact, it demonstrates the ongoing proposal to develop photovoltaic-related technologies, as research articles only accept results with a high degree of novelty. On the other hand, conference proceedings (papers) account for a persistently high proportion of publications, demonstrating efforts by organizations to hold frequent conferences and provide researchers with free space to discuss, present,

and publish their project outcomes. The large number of book chapters also indicate a publisher’s interest in sharing research resources that benefit readers’ learning

Table 2 reorganizes the article data by publisher, while Figure 5 illustrates the data in percentiles via a pie chart representation. Upon investigation, Springer is currently the publishing media that releases the most PV-related publications, covering everything from major research papers to minor editorials. Next came IEEE, Elsevier, and then MDPI, where they are all promising publishers in the engineering field. IEEE is known for its extensive conference proceedings around the world, while Elsevier and MDPI host numerous high-impact open access journals that contribute to knowledge dissemination. All participating publishers are striving to push PV-related technologies to the next level.

Table 2. Publisher’s publication count for specific article type.

Publisher	Scholarly Publication Count						Cumulative
	Research Paper	Review Paper	Book Chapter	Conference Paper	Editorial	Encyclopaedias	
Springer	22,769	9890	19,465	6866	0	1720	60,710
IEEE	8124	202	74	43,463	250	4	52,117
Elsevier	34,724	2547	1229	172	55	182	38,909
MDPI	6050	609	9	87	34	7	6796
ACS Publications	6474	102	19	132	0	0	6727
Wiley	5834	78	710	42	0	46	6710
AIP Publishing	3257	127	33	1316	47	7	4787
IOP Publishing	1702	123	1	1825	0	0	3651
Taylor & Francis	2214	78	0	0	1	0	2293
IET	984	19	82	608	0	0	1693
Hindawi	1304	65	0	6	12	0	1387
Inderscience	486	28	0	0	0	0	514
SAGE	351	20	1	94	0	0	466
MIT Press	47	66	140	0	0	2	255

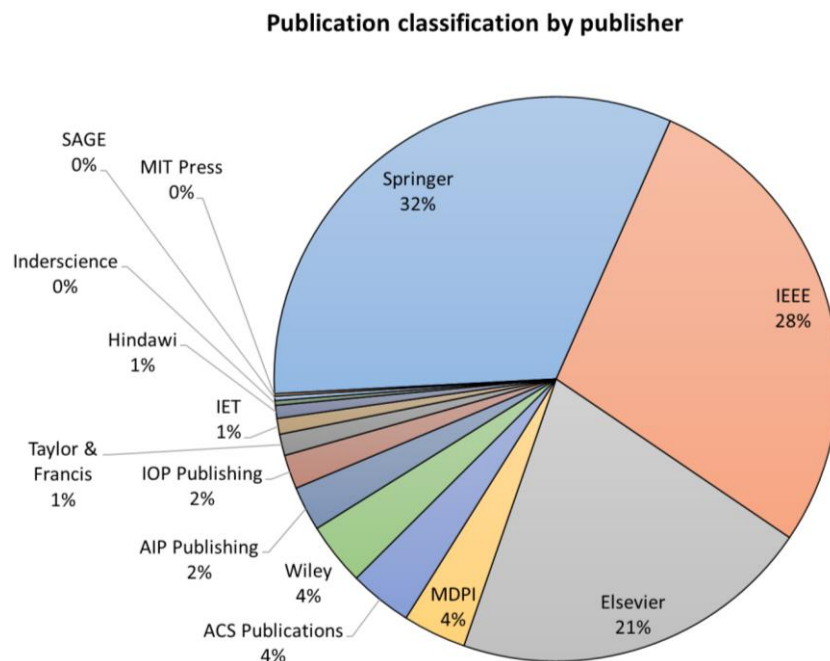


Figure 5. Proportion of publication classification by publisher.

The exact publication count by year, article type and publisher may be more than stated as the data presented is based only on information gathered through the outcomes of own review. However, the current amount of data is sufficient to provide key evidence

and reference for readers to comprehend the academic progress of PV-related publications over the years. It also advises researchers which publishers and article types would enable their studies to be recognized and accepted.

The use of solar energy is increasing worldwide and currently accounts for an estimated 5% of the world's electricity. However, global solar installations vary by country, with China having the largest installed solar capacity in the world, accounting for approximately 36% of the world's total energy production, followed by the United States at 11%, and Japan at 9%. According to experts, 133–175 gigawatts of new solar capacity were built globally in 2021, with another 200 gigawatts deployed by the end of 2022 [34]. This is clear evidence that solar energy has great potential for further expansion, as every country meets the geographic requirements to install solar technology. However, this review article is written for scholarly outreach purposes, and we prefer to review scholarly publications to reveal their distribution across countries. Table 3 exclusively records the relevant data, Figure 6 shows the data in the form of a pie chart, and Figure 7 displays the data in the form of a map chart. It is worth noting that China, United States and India are currently the top three countries with the largest number of proposals for photovoltaic-related articles in the global scale, of which China accounts for 20.84% of the total number of global academic publications, followed by the United States with 16.63% and India with 8.38%. Collectively, these three countries could have the most advanced knowledge in the installation, production and commercialization of solar power.

**Table 3.** Percentage distribution of scholarly publications by country.

Country	Distribution Percentage of Scholarly Publications
China	20.84%
United States	16.63%
India	8.38%
Germany	4.41%
South Korea	4.39%
Japan	4.34%
United Kingdom	4.22%
Italy	3.30%
Spain	3.04%
Australia	2.88%
France	2.76%
Iran	2.18%
Canada	2.15%
Malaysia	1.97%
Saudi Arabia	1.87%
Brazil	1.46%
Egypt	1.45%
Switzerland	1.31%
Turkey	1.25%
Singapore	1.19%
Other	9.98%

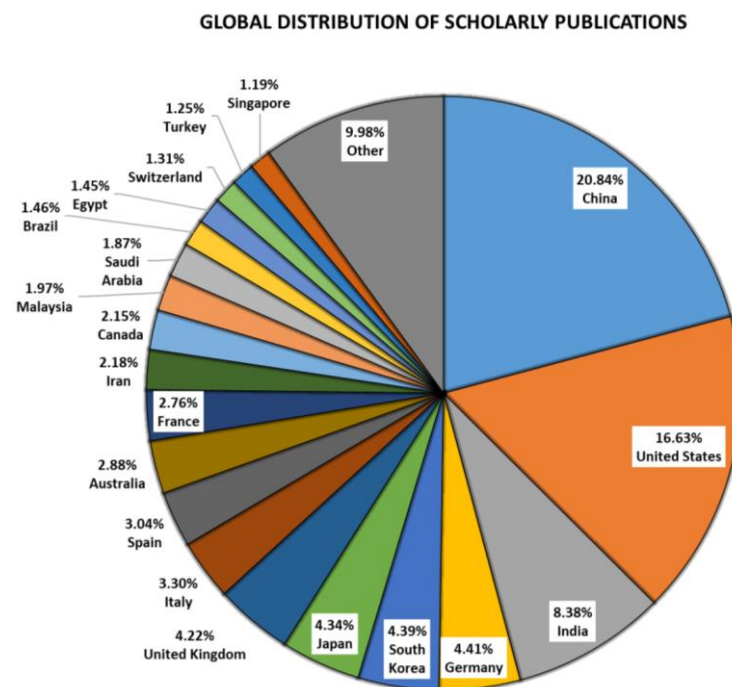


Figure 6. Proportion of publication classification by country.

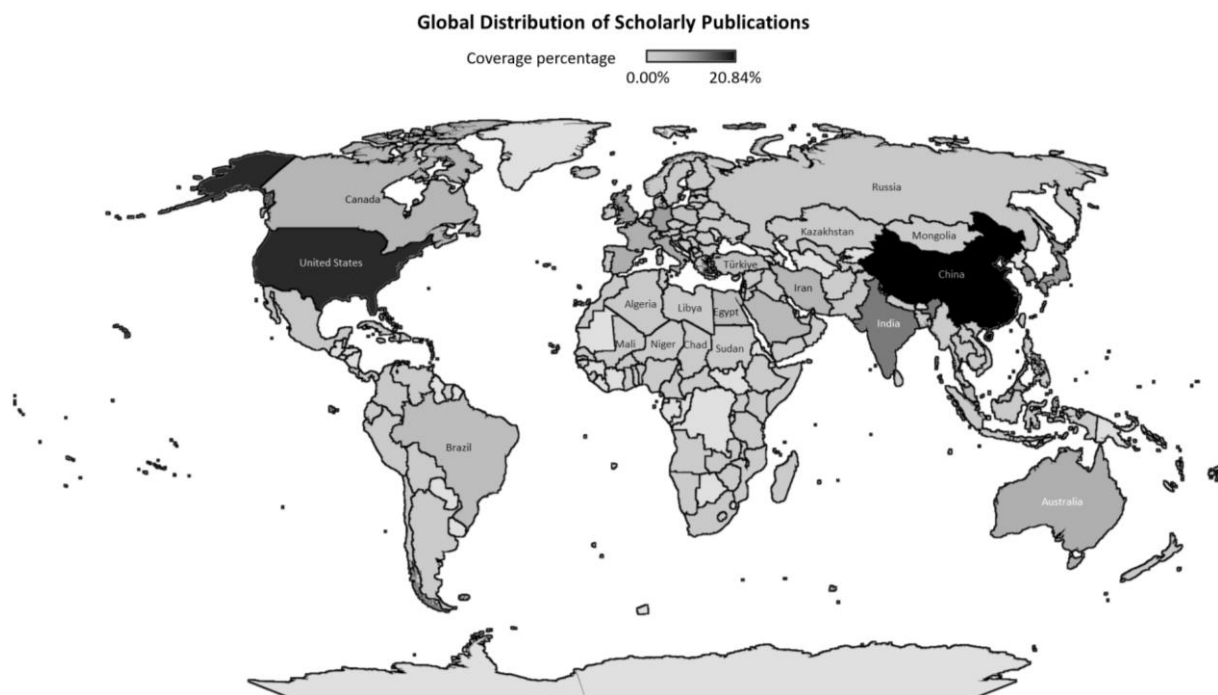


Figure 7. Global distribution of scholarly publications.

### 3. PV Panel

The PV panel is the main device that supplies electricity from solar energy, where the actual power-generating compound in the panel is the PV cell. Multiple PV cells are connected in series to establish a complete layer of PV modules, and multiple PV modules are connected in parallel and series to establish a complete PV array layer. In this review article, each compound is reviewed in an easy-to-understand order. To fully comprehend the architecture of a PV panel, one must study the mathematical concepts starting from the PV cell through to the PV array. Only then can the composition of the PV panel be

studied to understand the voltage, current and power performance under different shading degrees, connection patterns or both. Everything is thoroughly researched, including context, conditioning effects, and circuit flow patterns, where all explanations are fully supported figures, tables, and equations.

### 3.1. PV Cell

#### 3.1.1. Mathematical Modeling

PV cells are the smallest compound in the PV panel. It is essentially a diode made of semiconductors [35,36]. If a PV cell is short-circuited, the portion of cells exposed to sunlight generates charge carriers, which then generate current across the p–n junction [37,38]. Figure 8 depicts a common single-diode layout for a PV cell equivalent circuit [39–41]. In response to its layout, the  $I$ - $V$  characteristics of a practical PV cell can be expressed as follows [42,43]:

$$I_{pv,c} = I_{ph,c} - I_{sh,c} - I_{d,c} \quad (1)$$

where  $c$  denotes the index of PV cell,  $I_{pv}$  is the terminal current,  $I_{ph}$  is the photocurrent from the incident light, and  $I_d$  is the diode current. When light is incident on the PV cell, charge carriers transport across the p–n junction to generate  $I_{ph}$ . The value of  $I_{ph}$  depends directly on the irradiance level and the operating temperature. The generation of  $I_{ph}$  can be expressed mathematically as follows [44,45]:

$$I_{ph,c} = (I_{sc}^* + K_i \Delta T) \frac{G}{G^*} \quad (2)$$

where  $\Delta T = T - T^*$ ,  $T$  denotes the operating temperature of PV cell in Kelvin,  $T^*$  denotes the nominal operating temperature,  $G$  denotes the irradiance level in Watt per square,  $G^*$  denotes the nominal irradiance level,  $I_{sc}^*$  is the short-circuit current generated by projected sunlight underneath the nominal circumstance, and  $K_i$  is the temperature coefficient of short-circuit current ( $I_{sc}$ ). Note that the nominal condition is when irradiance level  $G = G^*$  and operating temperature  $T = T^*$ , where  $G^* = 1000 \text{ Wm}^{-2}$  and  $T^* = 298.15 \text{ K}$ , indicating the total exposure of cell's surface to solar radiation without any shaded region at the surrounding temperature of  $25^\circ \text{C}$ .

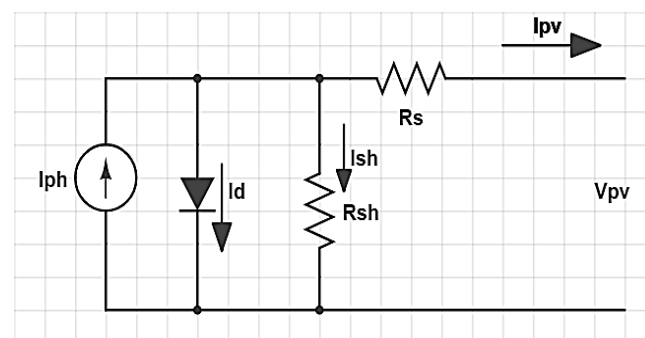


**Figure 8.** Internal layout of PV cell.

Meanwhile,  $I_{sh}$  can be simply calculated using the node voltage method, and the final expression is as follows:

$$I_{sh,c} = \frac{V_{pv,c} + I_{pv,c} R_s}{R_{sh}} \quad (3)$$

where  $V_{pv}$  is the terminal voltage,  $R_s$  is the series resistance, and  $R_{sh}$  is the shunt resistance.

At last, the diode current  $I_d$  can be expressed mathematically as follows [46]:

$$\begin{cases} I_{d,c} = I_o \left[ e^{\frac{q(V_{pv,c} + I_{pv,c}R_s)}{ak_bT}} - 1 \right] \\ I_o = I_o^* \left( \frac{T}{T^*} \right)^3 e^{\frac{qE_g}{ak_b} \left( \frac{1}{T^*} - \frac{1}{T} \right)} \\ I_o^* = \frac{I_{sc}^*}{e^{\left( \frac{V_{oc}^*}{aV_{T^*}} \right)} - 1} \end{cases} \quad (4)$$

where  $q = 1.60 \times 10^{-19}$  C denotes the electron charge,  $E_g$  indicates the band gap energy of semiconductor,  $a = 1$  denotes the diode ideality factor,  $k_b = 1.38 \times 10^{-23}$  JK<sup>-1</sup> denotes the Boltzmann constant,  $e()$  denotes the exponential function,  $I_o$  is the reverse saturation current,  $I_o^*$  is the reverse saturation current underneath the nominal circumstance,  $I_{sc}^*$  is the short-circuit current underneath the nominal circumstance,  $V_{oc}^*$  is the open-circuit voltage underneath the nominal circumstance, and  $V_{T^*} = k_b T^* / q$  denotes the thermal voltage of the PV cell at nominal temperature. Referring to Equation (4),  $I_o$  depends only on the temperature to calculate the diode current  $I_d$  [44,46].

Having identified the three  $I$  elements, we can substitute Equations (2)–(4) into Equation (1) to get the final formula for current generation in the PV cell:

$$I_{pv,c} = (I_{sc}^* + K_i \Delta T) \frac{G}{G^*} - \frac{V_{pv,c} + I_{pv,c}R_s}{R_{sh}} - I_o \left[ e^{\frac{q(V_{pv,c} + I_{pv,c}R_s)}{ak_bT}} - 1 \right] \quad (5)$$

According to Equation (5), changes in  $R_{sh}$  have little effect on the efficiency of the PV cell, whereas tiny changes in  $R_s$  have a significant impact. Therefore, in a real device, the value of  $R_s$  is set as low as possible and the value of  $R_{sh}$  is set as high as possible [39,47]. For ideal modelling,  $R_s$  is assumed to be short-circuited, while  $R_{sh}$  is assumed to be open-circuited, resulting in an ideal PV cell. In short, in an ideally designed PV cell,  $R_s = 0$  and  $R_{sh} = \infty$ . The shunt current  $I_{sh}$  is, hence, removed from the calculation because the current can no longer pass through  $R_{sh}$ . In this manner, the fundamental formula for an ideally constructed PV cell portrays the  $I$ - $V$  characteristics based on the semiconductor theorem [48]. Ideally, the terminal PV current  $I_{pv}$  is constituted only of  $I_{ph}$  and  $I_d$ , where  $I_{ph}$  supplies a portion of the current ( $I_d$ ) to the internal diode before transmitting it as  $I_{pv}$ .

### 3.1.2. Output Characteristics and Maximum Power Point

Note that the PV power  $P_{pv}$  produced by the PV solar cell is the product of  $I_{pv}$  and  $V_{pv}$ . It is a direct current (DC) type power supply. Figure 9 collect  $I$ - $V$  and  $P$ - $V$  characteristic curves from an ideally constructed PV cell, where SC indicates short-circuit status, and OC indicates open-circuit status [39,43]. They are the graphical curves that define the relationship between the current through the PV cell and the potential difference between its terminals. Combined with the explanation of the above mathematical formula, it can be inferred that the PV cell produces a nonlinear output effectiveness due to the intricate relationship between the overall resistance and the receiving temperature [49]. Figure 9 highlights three notable points, respectively, including the open circuit point at  $I_{pv} = 0$ , the short circuit point at  $V_{pv} = 0$ , and the maximum power point (MPP) at  $V_{pv} = V_{mp}$  and  $I_{pv} = I_{mp}$ . It is worth noting that the peak point of  $P_{pv}$  is represented as  $P_{mp}$ , where  $P_{mp}$  is the power value at MPP. It is mentioned in advance that MPP is the goal to achieve, which represents the global optimum of the maximum extractable output power of the PV model.

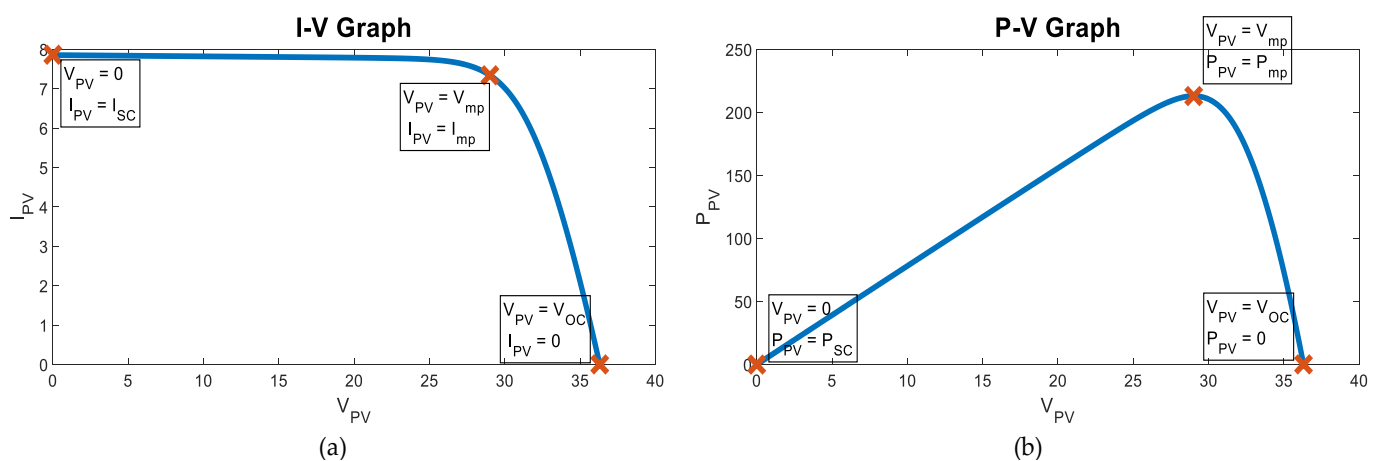


**Figure 9.** (a) *I-V* and (b) *P-V* characteristic curves of a PV module.

### 3.1.3. Solar Cell Technology in Generations

Photovoltaic solar cells can be composed of different materials to yield different energy conversion efficiencies. The physical and chemical properties of composite materials hugely determine the performance of photovoltaic cells. Hence, researchers have been working on developing innovative PV solar cells through continuous distribution, modification, reconfiguration, combination, dosage and any other chemical manipulations. Up to now, the photovoltaic solar cell companion has gone through four generations. Each has its own definitions and policies. The first generation of PV solar cells adopts crystallization technology, and is mostly made of silicon-based materials with thicker crystalline layers. It was the first product of its kind to hit the market in the solar sector, and now it has occupied 90% of the world-wide market share and 80% of the global installed capacity [50]. To save costs, second-generation PV solar cells replace silicon with thin-film technology to reduce the amount of material used while improving its quality. With the development of electrochemistry, the adopted materials were extended to copper indium gallium selenide (CIGS), cadmium telluride (CdTe), amorphous silicon (a-Si) and gallium arsenide (GaAs) [51,52]. The PV technology of third-generation solar cells is based on newer substances. By stacking new materials in thin layers, this generation of technology fills in the gaps of the second-generation technology and improves device efficiency [53]. The fourth generation is the latest generation. Solar cells from this generation are designed to boost solar cell efficiency and cost-effectiveness by combining inorganic and organic components. For better stability and endurance, they combine the benefits of earlier generations with cutting-edge organic nanomaterials including graphene, graphene derivatives, and carbon nanotubes [50,54].

There exist reliable aggregated data on the historical efficiencies of first to third-generation solar cells, but the efficiencies of fourth-generation solar cells over the years have yet to be sorted out by others. Hence, this review article endeavors to fill in the gaps left by others by completing an up-to-date list of efficiencies for first to fourth generation solar cells by category. With its efforts, this study aims to show the reader the rise of the fourth generation and its potential evolution in the near future. As part of the achievement, Table 4 records the summary of different material-based solar cells by generation, listing complete information on their efficiency, lifespan, cost and life cycle assessment.

Despite not having the superior energy conversion efficiencies at the current stage, it is self-evident that fourth-generation solar cells will continue to have strong growth expectations. So far, organic nanomaterials (i.e., graphene and carbon nanotubes) have been shown to be highly compatible with any solar cell of previous generations, leading to the intensive development of hybrid organic–inorganic nanocomposites for PV solar cells in recent years. [102,103]. Graphene, by definition, is a two-dimensional substance with a single layer of graphite, in which carbon atoms are organized into a hexagonal honeycomb lattice. Carbon nanotubes, on the other hand, are hollow cylinders in which sheets of

graphite are rolled into cylinders. Though both are composed of the same sub-material, they are taxonomically separable. Hence, they can be reasonably classified into three categories: graphene-based, carbon nanotube-based, and (combined) graphene/carbon nanotube or carbon nanotube/graphene-based, as shown in Table 4.

Even though graphene and carbon nanotubes are only as thick and heavy as a single atom, as they are made of a monoatomic layer of carbon atoms, they are characterized by their toughness, which is on par with diamond. These indeed endow the fourth-generation solar cells with high durability and lightness in the end-product. Furthermore, due to their ultra-thin layers, only minimal amounts of raw materials are required, which significantly reduces costs during the cell manufacturing process. As carbon is not hazardous to the environment, fourth-generation solar technology actually promotes cutting-edge green initiatives. Green disposal at the end of the product lifecycle is also conceivable, as nanomaterial-based solar cells have the potential to be made entirely of carbon through rigorous separation, purification, and enrichment methods that guarantee the inherent properties of pure carbon at ideal levels [104].

**Table 4.** Summary of efficiency, lifetime, cost and life cycle assessment of solar cells under the generation classification.

Material(s)-Based	Maximum Conversion Efficiency by the End of 2022 (%)	Estimated Lifespan (Years)	Manufacturing Cost	Environmental Indices	
				GHG (gCO <sub>2</sub> /kWh)	CED (MJ/m <sup>2</sup> )
<b>First-generation: crystalline silicon</b>					
Mono-crystalline silicon	27.6% [55]	25–40	\$0.34–0.54/W [56]	60.1–87.3 [57]	4200 [58]
Mono-crystalline silicon (concentrator)	26.1% [55]	25–50	\$0.30/W [59]	62–109 [60]	380–8700 [57]
Poly-crystalline silicon	23.3% [55]	14–35	\$1–2/W [61]	12.3–58.8 [57]	2544–3482 [62]
Heterostructure silicon	26.7% [55]	25–30	\$0.48–0.56/W [63]	47.5 [57]	3500 [64]
<b>Second-generation: thin-film</b>					
Copper indium gallium selenide (CIGS)	23.4% [55]	12–25	\$41–52/m <sup>2</sup> [56]	27 [65]	3005 [66]
CIGS (concentrator)	23.3% [55]	12–25	\$0.59/W [67]	NA	NA
Cadmium telluride (CdTe)	22.1% [55]	25–30	\$0.46/W [68]	14 [69]	81
Amorphous silicon (a-Si)	14.0% [55]	15–25	\$0.73/W [70]	20 [65]	989 [71]
Thin-film silicon	21.2% [55]	10–20	\$0.20/W [72]	36.9 [71]	NA
Mono-crystalline gallium arsenide (GaAs)	27.8% [55]	15–20	\$0.40/W [73]	NA	NA
GaAs (concentrator)	30.8% [55]	20–25	NA	NA	NA
Thin-film GaAs	29.1% [55]	10–15	\$0.50/W [74]	NA	NA
<b>Third-generation: emerging photovoltaic</b>					
Organic solar cells	18.2% [55]	10–20	\$48.80–138.90/m <sup>2</sup> [75]	37.8–56.7 [57]	96.7–125.0 [76]
Organic tandem solar cells	14.2% [55]	5–20	NA	5700–6000 [57]	43.9–51.3 [77]
Quantum dot solar cells	18.1% [55]	10–25	\$0.15–0.84/W [78]	5 [57]	1029.6 [57]
Perovskite solar cells	25.7% [55]	20–30	\$0.25–0.69/W [56]	147 [79]	504 [79]
Perovskite/Si tandem solar cells	31.3% [55]	15–29	\$121.18/m <sup>2</sup> [80]	46.4 [64]	NA
Perovskite/CIGS tandem solar cells	24.2% [55]	15–25	\$56.05/m <sup>2</sup> [81]	NA	NA
Dye-sensitized solar cells (DSSC)	13.0% [55]	5–7	\$22.40/m <sup>2</sup> [82]	22.4 [79]	277–365 [83]
Multi-junction solar cells	47.1% [55]	20–24	\$8.24/W [84]	40 [85]	860 [57]
Multi-junction solar cells (concentrator)	30.5% [55]	25–30	\$0.59/W [86]	NA	NA

Table 4. Cont.

Material(s)-Based	Maximum Conversion Efficiency by the End of 2022 (%)	Estimated Lifespan (Years)	Manufacturing Cost	Environmental Indices	
				GHG (gCO <sub>2</sub> /kWh)	CED (MJ/m <sup>2</sup> )
<b>Fourth-generation: nano photovoltaic</b>					
Graphene–silicon	18.8% [87]				
Graphene–quantum dot	13.7% [88]				
Graphene–perovskite	16.1% [89]				
Graphene/perovskite–quantum dot	17.9% [90]				
Graphene/quantum dot–perovskite	19.8% [91]				
Graphene–DSSC	11.5% [92]				
Carbon nanotubes–silicon	20.1% [93]				
Carbon nanotubes–quantum dot	6.00% [94]				
Carbon nanotubes–perovskite	37.4% [95]	0–1	TBD	TBD	TBD
Carbon nanotubes–DSSC	10.3% [96]				
Graphene/carbon nanotubes–silicon	17.5% [97]				
Carbon nanotubes/graphene–quantum dot	8.28% [98]				
Carbon nanotubes/silicon/graphene–quantum dot	14.9% [99]				
Graphene/carbon nanotubes–perovskite	19.6% [100]				
Carbon nanotubes/graphene–DSSC	8.34% [101]				

These organic nanomaterials are also highly flexible as they can take on other forms of structure [105]. With their flexibility, scientists have created a variety of solar cells that silicon cannot produce. This has led to unprecedented technological breakthroughs. Now, fourth-generation solar cells have been developed to prevent high local electric fields from hampering the electrical transport of surface charges. The synthetic nanomaterial sheets are physically transparent to a portion of infrared sunlight, which makes up around half of solar energy. These properties make them ideal for solar applications in aeronautical engineering, as they simplify installation via direct doping without compromising cell efficiency.

Nanotechnology has been widely used for structural reinforcement. As outcomes, products based on organic nanomaterials have been upgraded with higher electrical and thermal conductivity. More recently, it has been extended to solar technology to enhance the conductivity of PV cells in antistatic containers [106]. Since advanced nanotechnology can guarantee the good electrical conductivity of the synthesized nanomaterial sheet, it can act as a bridge to accelerate the transport of electrons from the metal derivative to the photoelectrode. With more promising thermal conductivity, fourth-generation solar cells convincingly address the major drawback of first and second-generation solar cells, which scorched the semiconductor lattice during operation. Nevertheless, the use of nanomaterials in solar cells contains a great deal of potential from the standpoint of electrothermal characteristics, and they are anticipated to be utilized in high energy-consuming sectors.

From the data collected in Table 4, we have enough information to reveal the merits and demerits of first to third-generation solar cells. Along with the understanding of the properties of organic nanomaterials, we can foresee the advantages and disadvantages

brought by the fourth-generation solar technology. To sum up, Table 5 summarizes the pros and cons of each generation of solar cells for better comparison, analysis and interpretation.

**Table 5.** Pros and cons [52–54] of solar cells explained under the generation classification.

Solar Generation	Pros	Cons
First-generation: crystalline silicon	<ol style="list-style-type: none"> <li>(1) Abundant mineral deposits in the Earth's crust ensure material availability</li> <li>(2) Non-toxic determination of pollution and durable retention</li> <li>(3) High compatibility</li> </ol>	<ol style="list-style-type: none"> <li>(1) Can be a bit expensive for large scale operations</li> <li>(2) Since silicon is an indirect bandgap semiconductor, it interacts weakly with light</li> <li>(3) Less tolerance for surface fouling as it causes significant power loss</li> </ol>
Second-generation: thin-film	<ol style="list-style-type: none"> <li>(1) Cheaper because less material is used to form micron-thick layers</li> <li>(2) Possess maximum absorption coefficient</li> <li>(3) Less production steps through direct integration into high-voltage modules</li> </ol>	<ol style="list-style-type: none"> <li>(1) Lower energy conversion efficiency</li> <li>(2) Rapid degradation to ambient light and therefore not preferable for outdoor applications</li> <li>(3) Limited availability of some materials</li> </ol>
Third-generation: emerging photovoltaic	<ol style="list-style-type: none"> <li>(1) Solution processable</li> <li>(2) Conducive to commercial production due to high efficiency at high temperature</li> <li>(3) Mechanically tough</li> </ol>	<ol style="list-style-type: none"> <li>(1) Solar power and manufacturing costs are high</li> </ol>
Fourth-generation: nano photovoltaic	<ol style="list-style-type: none"> <li>(1) Low cost</li> <li>(2) High flexibility, thus reducing industrial constraints</li> <li>(3) Very high toughness and hardness</li> <li>(4) High stability and durability</li> <li>(5) Lightweight and thin</li> <li>(6) Green initiatives</li> <li>(7) Physically transparent with minimal blocking of sunlight exposure</li> <li>(8) High electrical and thermal conductivity</li> <li>(9) Ease of preparation as materials are readily available</li> </ol>	<ol style="list-style-type: none"> <li>(1) Very short lifespan</li> <li>(2) Incomplete research resources lead to insufficient practical integrity</li> <li>(3) Commercialization is speculative due to insufficient evidence of commercial validity</li> </ol>

Upon discussion, the market of the first generation of solar cells has been saturated due to earlier commercialization. Despite every effort to maximize efficiency, further development of the first generation is expected to face some challenges, as the pristine nature of silicon interacts weakly with light and is less resistant to significant power losses. Second-generation solar technology is not satisfactory due to the limited availability of certain materials, not to mention its biggest drawback is rapid degradation to ambient light, making it unsuitable for outdoor applications. However, the third-generation solar technology has achieved higher breakthroughs, mainly perovskite and multi-junction cells whose efficiencies are 5.4% and 21.2% higher than the average efficiency of the first-generation solar technology, and the overall efficiency is also 0.7% higher than that of the second-generation solar technology. For now, third-generation solar technology has indeed taken over the research market. Hence, the subject will turn to whether the fourth-generation solar technology has the potential to surpass the third generation in terms of the suitability of energy supply and the stability of commercialization. Due to the aforementioned advantages brought about by the excellent properties of nanomaterials, and their ability to be integrated with any type of previous-generation solar cells, the peak efficiencies of fourth-generation solar cells are rapidly increasing, though the technology is still in its infancy and early stages of development. With advances in materials engineering, pathways to improve panel efficiency will be realized.

Accordingly, first and second-generation solar technologies are expected to be commercially replaced by third and fourth-generation technologies. To eliminate existing solar cells, proper recycling and disposal methods must be implemented. Recycling is more preferable to minimize cost and waste of material, while solar cell disposal with minimal impact on the environment also needs to be considered. Notably, waste from end-of-life solar panels can present the opportunity to recover valuable materials through recycling and reprocessing. The International Renewable Energy Agency predicts that by 2030, the cumulative value of recycled raw materials used in end-of-life panels will be about \$450 million, equivalent to the price of raw materials needed to make about 60 million new panels [107]. Fortunately, most of the components in first and second-generation solar cells can be recycled. The composition of monolithic solar cells is generally glass, aluminum and rare metals, such as silicon, indium gallium, arsenic, etc., among which the rare metals with the highest content determine the naming of solar cells. Table 6 collects recycling data for first and second-generation solar cells. These findings could provide avenues for efficient material recovery.

**Table 6.** Solar waste recycling information [108–111].

Generation	Solar Cell	Recyclable Material	Recovery Rate (%)	
First	Silicon-based	Aluminum	100	
		Glass	95	
		Silicon	85	
Second	GICS-based	Aluminum	100	
		Glass	95	
		Indium	90	
		Gallium	90	
		Copper	90	
	CdTe-based	Aluminum	100	
Glass		90		
GaAs-based	CdTe-based	Cadmium telluride semiconductor	95	
		GaAs-based	Aluminum	100
			Glass	95
			Gallium	98
			Arsenic	98

In any case, the biggest challenge facing fourth-generation solar technology is how to extend the lifespan of fourth-generation solar cells. At present, the product lifespan of the technology is expected to be as long as one year, which is too short for stable commercialization. One of the possible major solutions could be further breakthroughs in the quality of materials, but this could be accompanied by developments in materials science that usually require considerable time and expense to accomplish. Another option can be chemical processing, which requires a deep understanding of chemical science, including acid treatment, coating, doping, etc. to enhance the durability, sustainability and conductivity of solar materials. Instead, physical improvements to the solar panels may be the most effective solution, as running solar photovoltaic cells at cooler temperatures has been shown to extend their lifespan. So far, researchers have proposed and tested several cooling techniques for panels. One of the most common and effective coolants is water [112]. The following literature [113] is cited for any possible breakthroughs in cooling techniques in response to recent solar research. These findings may provide avenues for the efficient development of fourth-generation solar technology in the future.

All these claims support the bright future of fourth-generation solar cells, which are expected to account for half of the research market in the coming years. However, this generation of solar cells still faces certain insufficiencies. Another challenge lies in determining the proportional concentration of nanomaterials used in the solar cell. Improper rationing can lead to defects that instead assimilate light from the solar cells, reducing the energy

conversion efficiency of the solar cell [114,115]. Hence, it is foreseeable that researchers will continue to put in more efforts to overcome this challenge and contribute to the further evolution of more efficient PV solar cells.

### 3.2. PV Panel

#### 3.2.1. Mathematical Modeling

A PV panel is generally regarded as a single PV array, where a PV array is composed of  $N_p$  PV modules in parallel and  $N_s$  PV modules in series, and a PV module consists of  $N_c$  PV cells connected in series.

A PV module is typically where PV cells are connected in  $N_c$  series, where  $N_c$  is specified as the PV cell number per module string. Every electronic component in a series-connected circuit receives the same amount of electric current, as there is just one possible route for current to bypass. Instead, every electronic component has different potential difference (voltage) based on its resistance value, and, hence, the sum of the voltage drops at all electronic components in a series circuit constitutes the total voltage. In a PV module, the voltage produced by each PV cell should be aggregated while the current remains equal, so the expressions for the PV terminal voltage and current of a single PV module can be derived as follows:

$$\begin{cases} V_{pv,c} &= \frac{V_{pv,m}}{N_c} \\ I_{pv,c} &= I_{pv,m} \end{cases} \quad (6)$$

where  $m$  denotes the index of PV module.

By extension, a PV array is where PV modules are typically connected in  $N_p$  parallel and  $N_s$  series, where  $N_s$  denotes the module number per array string and  $N_p$  denotes the array string (parallel) number. PV modules in series provide greater output voltage, and PV array strings in parallel increase output current [39], so the expressions of the PV terminal voltage and current of a single PV array can be derived as follows:

$$\begin{cases} V_{pv,m} &= \frac{V_{pv,a}}{N_s} \\ I_{pv,m} &= \frac{I_{pv,a}}{N_p} \end{cases} \quad (7)$$

where  $a$  denotes the index of PV array. By substituting Equations (6) and (7) into Equation (5), the  $I$ - $V$  characteristics of a practical PV array can be obtained as follows [47]:

$$I_{pv,a} = N_p (I_{sc}^* + K_i \Delta T) \frac{G}{G^*} - \frac{N_p V_{pv,a} + N_s N_c I_{pv,a} R_s}{N_s N_c R_{sh}} - N_p I_0 \left[ e^{\frac{q(N_p V_{pv,a} + N_s N_c I_{pv,a} R_s)}{N_s N_p N_c a k_b T}} - 1 \right] \quad (8)$$

#### 3.2.2. Impact of Partial Shading Condition on PV array

As analyzed from the mathematical modelling, the operating temperature  $T$  and irradiance level  $G$  in a PV module determine the PV output power. Note that the operating temperature is uniform because every PV cell is exposed underneath the same environment and shares the same ambient temperature. However, sometimes when the sunlight is blocked, the surface of the PV cells may be shaded to a certain extent, so the PV module cannot receive the full irradiance but only a certain percentage.

If uneven shading occurs on a PV panel of an array with multiple PV modules connected in series, this will result in different PV modules receiving varying irradiance levels in the panel. This is the so-called partial shading phenomenon [116]. Figure 10 displays the  $I$ - $V$  and  $P$ - $V$  characteristic curves of PV panel underneath partial shading condition, where the PV panel (or array) has five PV modules connected in series, each with irradiance levels set at 1000, 800, 600, 400 and 200 W/m<sup>2</sup>, at a nominal temperature of 25 °C. Given the different percentages of shading in each module, there appear to be five peaks on the  $P$ - $V$  curve. The middle peak with the highest  $P_{pv}$  value approximately equal to 420 W is the MPP, where this value is the global optimal power (i.e.,  $P_{mp}$ ) that the PV panel can produce. The remaining peaks other than MPP are local maxima, which produce power

peaks somewhat lower than MPP. Nonetheless, MPP is the only optimization objective to obtain maximum PV power.

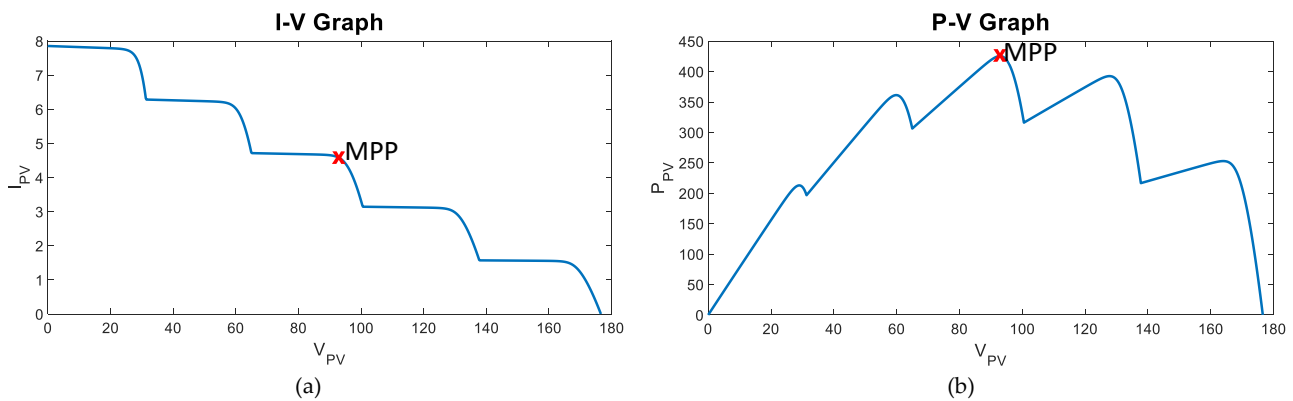


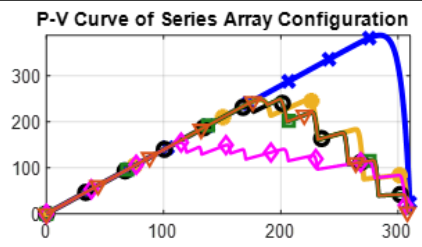
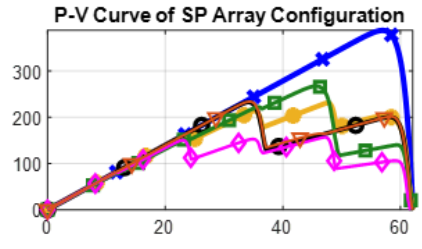
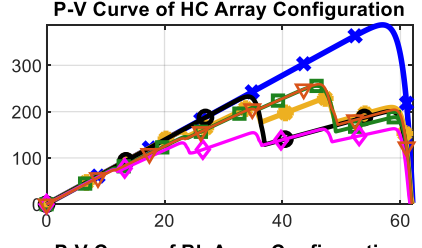
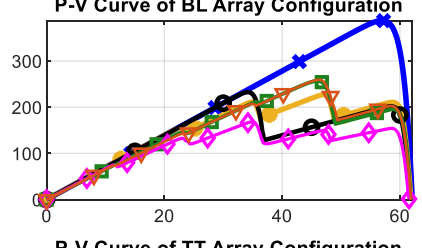
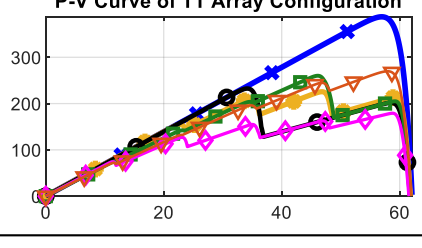
**Figure 10.** (a) *I-V* and (b) *P-V* characteristic curves of PV panel underneath partial shading condition.

In theory, a PV module that is shaded would never extract more current than another module that is not shaded, and, hence, the amount of extractable current decreases along with the shading percentage. The following statement will explain the composition of the peaks in the *P-V* curve [117]. Note that each PV module is connected in parallel with a diode. When the current is less than or equal to 1.58 A, it bypasses all five PV modules. When the current is less than or equal to 3.16 A but greater than 1.58 A, it bypasses the four PV modules but forward biases the diode in parallel with the 200 W/m<sup>2</sup> irradiated PV module. When the current is less than or equal to 4.74 A but greater than 3.16 A, it bypasses the three PV modules but forward biases the diodes in parallel with the 200 W/m<sup>2</sup> and 400 W/m<sup>2</sup> irradiated PV modules. When the current is less than or equal to 6.32 A but greater than 4.74 A, it bypasses the two PV modules but forward biases the diodes in parallel with the 200 W/m<sup>2</sup>, 400 W/m<sup>2</sup> and 600 W/m<sup>2</sup> irradiated PV modules. When the current is less than or equal to 7.90 A but greater than 6.32 A, it bypasses only one PV modules but forward biases the diodes in parallel with the 200 W/m<sup>2</sup>, 400 W/m<sup>2</sup>, 600 W/m<sup>2</sup> and 800 W/m<sup>2</sup> irradiated PV modules [118]. When current bypasses the diodes, these modules are open-circuited, and no voltage is generated. This, hence, reduces the sum of the voltages at the panel terminals. These analyses of the *I-V* characteristic curve (in Figure 10) provide the supporting statements for these findings.

### 3.2.3. PV Array Configuration

Providing efficient energy for photovoltaic power generation systems is always a major concern. Note, however, that there are some significant challenges in maximizing the output power of a PV solar array. One of the main challenges is partial shading conditions, which can lead to poor output power due to power loss mismatch between PV modules. Upon investigation, it can be confirmed that these losses are closely related to the structure of the PV system, the shading patterns, and the configuration of the PV array. Since the shading patterns are just settings that simulate the physical position and tilt angle of the shaded PV modules in a hardware setup, they are merely samples for experimental testing. Instead, PV array configurations are crucial to harvest maximum power in centralized topologies. This has encouraged researchers to exploit the potential of various PV array configurations to achieve more stable, robust and efficient power generation from PV panels. The research outcomes are shown in Figure 11. As the research progresses, we document in Table 7 the output characteristics and efficiencies for different array configurations under various shading effects.

**Table 7.** Summary of output characteristics and efficiencies for different array configurations in various shading patterns.

PV Array Configuration	Efficiency in Different Shading Patterns					P-V Output Characteristic
	Center	Bottom	L-Shaped	Random	Diagonal	
Series	64.16%	63.98%	64.30%	40.00%	64.30%	
Series-Parallel (SP)	59.53%	60.00%	68.91%	40.42%	60.30%	
Honeycomb (HC)	58.99%	60.00%	65.96%	42.09%	66.91%	
Bridge-Link (BL)	58.60%	60.00%	66.24%	43.39%	66.94%	
Triple-Tied (TT)	58.21%	60.00%	67.13%	46.23%	69.63%	

● Uniform (non-shaded)
 ● Center
 ● Bottom
 ■ L-shaped
 ◆ Random
 ▲ Diagonal
 , Efficiency :  $\frac{P_{mp,shaded}}{P_{mp,uniform}}$

From the data collected in Table 7, we can analyze the strengths and weaknesses of each PV array configuration. Table 8 summarizes our discussion. It can be inferred that TT configuration has the best performance and stability compared to other reviewed PV array configurations, which is probably the best solution against the impacts of partial shading conditions. In practice, however, it is difficult to determine which is the most suitable in general, as each array configuration has its suitability depending on the situation and user requirements. From an in-depth discussion, we conclude that research on PV array configurations has reached certain limitations. Further development of PV array configurations will slow down in the coming years, but the challenge still lies in how

to efficiently and sustainably harvest maximum power with small relative errors under load-bearing environmental conditions.

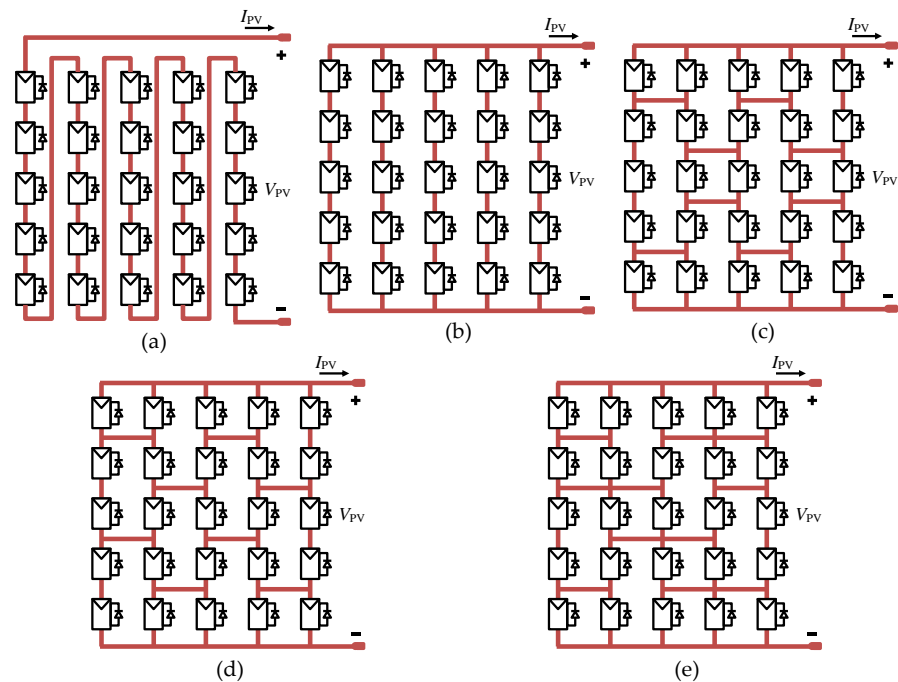


**Figure 11.** PV array configuration models: (a) series, (b) series-parallel (SP), (c) honeycomb (HC), (d) bridge-link (BL), (e) triple-tied (TT).

**Table 8.** Overview of PV array configurations with their pros and cons [119,120].

PV Array Configuration	Merits	Demerits	Remark
Series	(1) Involves minimal cabling, thereby reducing cabling losses (2) Vulnerable to aging	(1) Very high mismatch power loss	It consists of the greatest number of series connected PV modules. Hence, it has the worst ability to achieve maximum power due to the highest numbers of power peaks produced under highly complex partial shading conditions.
Series-Parallel (SP)	(1) Ease of construction as there are no redundant connections (2) Economical (3) Vulnerable to aging	(1) High mismatch power losses due to long series connections in the strings	It consists of a larger number of series connected PV modules. Hence, it is relatively less capable of achieving maximum power due to the highest numbers of power peaks produced under highly complex partial shading conditions.
Honey-Comb (HC)	(1) Less susceptible to mismatch power losses than SP configurations since it consists of a smaller number of PV modules connected in series (2) Higher stability in response to environmental changes than SP configurations (3) Longer service life (4) Preferred for grid-connected central inverters and stand-alone PV systems	(1) High cabling costs and high cabling losses as extra cables are required in cross-connects (2) High redundancy	It consists of a moderate number of PV modules connected in series. As a result, it has modest maximum power-achievement capabilities due to a decent amount of power peaking under highly complex partial shading conditions.

Table 8. Cont.

PV Array Configuration	Merits	Demerits	Remark
Bridge-Link (BL)	(1) Less susceptible to mismatch power losses than HC configurations since it consists of a smaller number of PV modules connected in series (2) Higher stability in response to environmental changes than HC configurations (3) Longer service life	(1) High cabling costs and high cabling losses as extra cables are required in cross-connects (2) High redundancy	It consists of a smaller number of PV modules connected in series. Therefore, it has a relatively good ability to achieve maximum power due to fewer power peaks generated under highly complex partial shading conditions.
Triple-Tied (TT)	(1) Least susceptible to mismatch power losses as it consists of the least number of PV modules connected in series (2) Has the most superior and powerful performance than other PV array configurations (3) Longest service life	(1) Very high wiring cost and very high wiring losses, as there are more complex cross-connects, so more cables are required (2) Very high redundancy	It consists of the least number of PV modules connected in series. Hence, it has the best ability to achieve maximum power due to the least number of power peaks produced under highly complex partial shading conditions.

#### 4. Controller

##### 4.1. Working Principles Related to Other Devices

The controller is an electronic device that controls the circulating circuits in a PV system to collect as much power as possible from the solar panel. The internal layout of the controller can refer to Figure 1. The controller basically consists of a maximum power point tracking (MPPT) module and a pulse wave modulation (PWM) generator. In fact, the controller's MPPT module serves a crucial role, as it applies the body specifying the MPPT technique to optimize certain vital parameters at runtime, in an attempt to find a better solution for greater power extraction from the PV panel, until the end of the iteration [121]. By definition, MPPT is the process of controlling the system to achieve the MPP (i.e.,  $P_{mp}$ ) in the  $P$ - $V$  characteristics of the PV panel, where all intelligent methods or optimization algorithms for tracking, searching and reaching  $P_{mp}$  are regarded as MPPT techniques [122]. The MPPT technique tunes the duty cycle  $D$  while referencing the inputs measured from the terminals of PV panel (i.e.,  $V_{PV}$  and  $I_{PV}$ ) or environment (i.e.,  $G$  and  $T$ ). The PWM generator then receives the tuned duty cycle  $D$  to create the desired structure in the PWM signal  $S$ . Note that a PWM signal is a digital pulse consisting of only "ON" or "OFF" data.  $D$  varies from 0 to 1, representing the ratio of continuous "ON" intervals to a given time period. Figure 12 shows the graphical structure of the PWM signal  $S$  for different  $D$  values, when  $D$  is equal to 0.25, 0.5 and 0.75, respectively. From Figure 12, it can be deduced that  $D$  also represents a percentage in decimal format. As we expand the explanation,  $S$  remains fully "ON" when  $D$  is equal to 1, and it becomes completely "OFF" when  $D$  is equal 0. Typically, the operating frequency of the PWM generator is preferably set to  $>1000$  Hz to speed up the regulation process in the converter block. The digital PWM signal  $S$  will then be sent as a controlling signal to the boost converter to alter the PV power extraction (from the PV panel).

To avoid confusion, we must specify that the controller is the device that indirectly controls the amount of PV power ( $P_{pv}$ ) that the boost converter can extract and stabilize. We define the maximum available power obtained by the load  $R$  in the converter as  $P_{max}$ , where  $P_{max} = P_R$  when  $t > t_{max}$ ,  $t$  is the index of iteration, and  $t_{max}$  is the total number of iterations (generations) adopted by the installed MPPT technique. Theoretically,  $P_{pv} \approx P_R$  at any moment due to the effective stabilization of the boost converter, and hence, tuning solution  $D$  for better  $P_{pv}$  using any MPPT technique indicates the effort to achieve the optimal  $P_R$  value in the process. This also brings the same implication that the MPPT module aims to help the PV system to obtain  $P_{max}$  that is preferably near to or equivalent

to  $P_{mp}$  in  $P$ - $V$  characteristic curve. Therefore, the evaluation metric of the controller can be expressed as:

$$RE_{\%} = \frac{P_{mp} - P_{max}}{P_{max}} \times 100\% \quad (9)$$

where  $RE_{\%}$  relative percentage error. In fact,  $P_{max} \leq P_{mp}$ , the narrower the difference between  $P_{max}$  and  $P_{mp}$ , the less the  $RE_{\%}$ , and consequently, the higher the efficiency and performance of the MPPT technique, thus ensuring satisfactory power supply to the end-user [123]. That is all the mechanics and relationships of the MPPT process we claim to be played by the controller block.

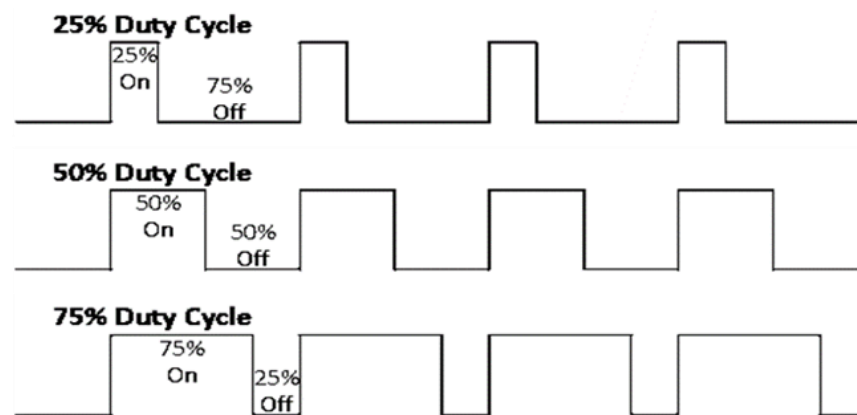


**Figure 12.** PWM signal S generated by different scenarios.

#### 4.2. MPPT Techniques and Classification

MPPT techniques have continued to develop over the years. Upon survey, novel MPPT techniques are expected to replace conventional MPPT techniques in the future to address the significant shortcomings of conventional MPPT techniques that lack precise localization of the MPP due to persistent oscillations around the MPP. For validation, this review article exclusively cites 20 novel MPPT techniques and expands further taxonomy for ease of classification to provide evidence as to which class of MPPT is currently receiving the most attention and achievement during these years (2019–2022). Table 9 collects the information about them. This study investigates the development direction of MPPT techniques in these few years, so as to ease the process of prediction for future challenges.

**Table 9.** Hierarchical development and applications of MPPT techniques under the complete MPPT classification from 2019 to 2022.

MPPT Classification	Sub-Genre	MPPT Technique Based on:	Ref.	Year
Classical	NA	Perturb and observe (P&O)	[124]	2020
		Incremental conductance	[125]	2020
		Ripple correlation	[126]	2020
Intelligence	NA	Artificial neural network-assisted sequential Monte Carlo (ANN-SMC)	[127]	2019
		Resilient backpropagation-neural network (Rprop-NN)	[128]	2019
		Quantum neural network (QNN)	[129]	2022
		Fuzzy logic control (FLC)	[130]	2022

Table 9. Cont.

MPPT Classification	Sub-Genre	MPPT Technique Based on:	Ref.	Year
Optimization	Basic optimization	Peafowl optimization algorithm (POA)	[131]	2021
		Mayfly algorithm (MA)	[132]	2022
		Remora optimization algorithm (ROA)	[133]	2022
	Modified or improved optimization	Improved cuckoo search (ICS) algorithm	[134]	2021
		Modified normative fish swarm algorithm (mNFSA)	[135]	2022
		Modified seagull optimization algorithm (MSOA)	[136]	2022
	Hybrid optimization	Genetic algorithm (GA) and ant colony optimization (ACO)	[137]	2021
		Particle swarm optimization (PSO) and salp swarm optimization (SSO) algorithms	[138]	2022
	Hybrid	Classical–Intelligence	NA	
Classical–Optimization		NA		
Intelligence–Optimization		Adaptive neuro-fuzzy inference system and artificial bee colony (ANFIS–ABC)	[139]	2019
		Artificial neural network and particle swarm optimization (ANN–PSO)	[140]	2020
		Adaptive neuro-fuzzy inference system and particle swarm optimization (ANFIS–PSO)	[141]	2020
		Genetic algorithm and artificial neural network (GA–ANN) with genetic algorithm/particle swarm optimization and fuzzy logic control (GA/PSO–FLC)	[142]	2021
		Modified firefly algorithm, adaptive neuro-fuzzy inference system, and perturbation and observation (MFA–ANFIS–P&O)	[143]	2020

Throughout the course of the inquiry, we discovered that numerous novel MPPT techniques inspired by various intelligent approaches and metaheuristic optimization algorithms provide more efficient solutions than existing traditional MPPT techniques. In addition, the latest innovations in MPPT technology have been made possible by deeply revamping, modifying and hybridizing existing MPPT techniques of different classes. It is believed that formidable intelligent methods and algorithms are inherently sufficient to search, discover, and reach the MPP, even for direct MPPT applications in PV systems.

As can be seen from the overview (in Table 9), all cited MPPT techniques were classified into 4 categories: classical, intelligent, optimization, and hybrid MPPTs. Classical MPPT techniques were starting to fall behind their development process. Intelligence MPPT and hybrid MPPT techniques somewhat remain growing. On the other hand, optimization MPPT definitely accounted for the largest number of proposals since 2021. Optimization MPPT has indeed received more attention than other classified MPPTs in recent years. Obviously, from 2021, researchers start to switch the concern of the development to the optimization MPPT techniques. All these combined facts indicate that the optimization MPPT techniques can be the best compatible to the photovoltaic applications. In-depth

research on optimization MPPT is expected to be a near-term trend, at least in the future 5 years.

The extensive research resources (in 2021–2022) make it possible to further divide optimization MPPT into three subcategories: basic optimization MPPT, modified optimization MPPT, and hybrid optimization MPPT. Optimization MPPT techniques are basically modeled with reference to these sub-genres of nature-inspired metaheuristic optimization algorithms. From here, we can boldly deduce that the rise of optimization MPPT techniques accompany along with the recent high popularity of optimization algorithms in the field of mathematical computing. So far, it is noticeable that the number of proposals for novel optimization algorithms have been significantly increasing over the years, especially since 2020. From survey, these newly proposed algorithms can generally fall into three broad categories: bio-inspired, physics-based, and evolution-based [144]. Note that most of the optimization MPPT techniques cited under these subcategories are of the bio-inspired type, which shows how compatible biomimetic algorithms are in MPPT applications. Since biomimetic metaheuristics are the latest trending candidates in MPPT applications, we set out to search for any potential novel bio-inspired algorithms, hoping to get some leading information in this field. Through further investigation, we discovered these potential bio-inspired metaheuristic optimization algorithm: In 2022, Mountain Gazelle Optimizer (MGO) [145], Artificial Rabbits Optimization (ARO) algorithm [146], Dandelion Optimizer (DO) [147], Dwarf Mongoose Optimization Algorithm (DMOA) [148] and Pelican Optimization Algorithm (POA) [149] were proposed. In 2021, Dingoes Optimization Algorithm (DOA) [150] and African Vultures Optimization Algorithm (AVOA) [151] were proposed. In 2020, Black Widow Optimization (BWO) algorithm [152] and Mayfly Algorithm (MA) [153] were proposed. In 2019, Emperor Penguins Colony (EPC) algorithm [154], Harris Hawks Optimization (HHO) algorithm [155], Artificial Coronary Circulation System (ACCS) algorithm [156], Blue Monkey (BM) algorithm [157] and Sunflower Optimization (SFO) algorithm [158] were proposed. Any of these are likely to be the better solutions for MPPT applications for years to come.

## 5. DC-DC Boost Converter

### 5.1. Working Principles Related to Other Devices

In essence, a converter is an electromechanical device that converts alternating current (AC) to direct current (DC), whereas an inverter is an electromechanical device that converts direct current (DC) to alternating current (AC). DC is characterized by the fact that the polarity of the current does not change with time, while AC refers to the magnitude and polarity (orientation) of the current changes with time. In a PV application system, the considerable device that draws electricity from the attached PV panel is the boost converter, where it is supposed to radially connect to the PV panel. It behaves to regulate PV panel output while interrogating the incoming PWM signal  $S$  [159]. Since the power generation of PV cells is DC type, most semiconductor devices can only work with DC [160]. Generally, there are two classifications of DC–DC converter types such as isolated and non-isolated DC–DC converters. The isolated DC–DC converter uses a transformer to step-up or step-down the input voltage, while the non-isolated DC–DC converter uses semiconductor components for voltage conversion, with smaller volume and higher efficiency [161,162]. As we go deeper into the comparison, non-isolated high-boost DC–DC converters have less magnetic losses and are less expensive. These factors ease construction and make the non-isolated converters economical in terms of manufacturing and maintenance costs. Hence, non-isolated DC–DC converters are always preferred over isolated DC–DC converters in photovoltaic applications.

PV power sources (that is, PV panel) generally output a low voltage of 12~60 V, so an adjoined DC–DC converter with a high output voltage gain is imperative to make the entire PV system more suitable for 375~760 V grid-connected applications [163–165]. Hence, a non-isolated DC–DC converter with low current-ripple and voltage conversion ratio greater than 10 is the best choice as it reduces losses and improves operating efficiency. It

is worth noting, however, that many of the DC–DC converter topologies presented in the literature that provide high voltage gain are regularly made for power levels below 1 kW. This is due to the fact that converters with high output power levels can severely burden the research process by raising the expense and risk of the experiment during the hardware setup [166,167]. Combining all statements and facts, non-isolated high-gain low-power (HGLP) DC–DC converters are currently the best candidates for PV-related applications. DC–DC boost converters fall into this category and are the most suitable and commonly used converters for these applications.

Integrated circuits (ICs) and other components mounted on substrates used in kits have specific operating voltage ranges and require different voltage accuracy. Unstable or improper voltage supply can lead to characteristic degradation or even failure. To prevent this, a boost converter is usually required to convert and stabilize the voltage, and so a device that use a boost converter to stabilize the voltage are called voltage regulator [168]. Voltage regulation is primarily handled by a transformer at the center of the converter, which specializes in amplifying the voltage and reducing the current flowing to the load (end-user), while maintaining constant electrical power.

The layout of a conventional boost converter can be referred to Figure 1. The boost inductor (L), the diode, the DC bus capacitor (C2), and the metal oxide semiconductor field effect transistor (MOSFET) make up a DC–DC boost converter [169,170]. Beyond it, the load (R) and filter capacitor (C1) also play important roles, where the load R stands for the user end.

The two capacitors, C1 and C2 play the major role in maintaining voltage stability via charging and discharging, the process of which is mainly controlled by the PWM signal S. If S sends an “ON” signal, the MOSFET is toggled “ON”, otherwise the MOSFET is toggled “OFF”. When the MOSFET is toggled “OFF” it acts as an open-circuit path, where current bypasses all components including C1, C2, L and R. The fully connected circuit charges C1 and C2 at this point. Note that a fully discharged capacitor acts as a short circuit (current with no voltage drop), while a fully charged capacitor acts as an open circuit (voltage drop with no current). From the layout, we know that  $V_{pv} = V_{c1}$  and  $V_R = V_{c2}$ , where  $V_R$  denotes the voltage collected from the load R. In theory, more current can be drawn from the PV panel (power supply) when the circuit resistance is lower. Conversely, when the MOSFET is toggled “ON”, it acts as a short-circuit path, allowing maximum possible current bypass. Due to the laws of physics, current will flow through a circuit path with negligible resistance, so most of the PV current ( $I_{pv}$ ) drawn from the panel will not pass through the C1 component, but rather flows almost entirely to the short-circuit path created by the MOSFET. Therefore, at this moment, C1 begins to discharge an upward current to the node. More directly, the capacitor discharges when short-circuited. The current discharged by C1 ( $I_{c1}$ ) will then be summed with  $I_{pv}$  and sent to the short-circuit path. This corresponds to the fact that  $V_{c1}$  gradually drops to zero when the MOSFET is toggled “ON”. Meanwhile C2 is solely responsible for discharging its voltage and current to the load R, as the circuit has already been separated. This helps to temporarily maintain the voltage and current supplied to the user without huge oscillations [171].

In converter, the role of the inductor L is to generate an electromotive force in the direction to reduce the fluctuation when a fluctuating current flows, helping to stabilize the current and voltage in the system [170]. From the moment the MOSFET is toggled “ON”, the current flowing through the inductor L increases, the inductor L starts to store energy in the magnetic field. During this process, the potential across inductor L will be negative at the right and positive at the left, where the positive sign of the PV panel is connected to the positive sign of inductor L. This temporarily hinders the bypass of  $I_{pv}$ . However, after a moment, when the inductor L reaches steady state during energy storage, it becomes an ideal zero resistance element, allowing almost 100%  $I_{pv}$  bypassing without dropping any potential difference. When the MOSFET is turned “OFF”, the circuit resistance increases and the panel no longer outputs large current at the terminals. The  $I_{pv}$  drops and the inductor L begins to release energy. At this point, the potential across the inductor L will

be positive at the right and negative at the left. Since the positive sign of the PV panel is connected to the negative sign of the inductor  $L$ , the total voltage supplied to the load  $R$  is an added value. Therefore,  $C_2$  can be charged underneath the greater potential difference. Through further analysis, we can deduce that the maximum  $V_{C_2}$  (i.e.,  $V_R$ ) value is much higher than that of  $V_{C_1}$  (i.e.,  $V_{pv}$ ) [172]. Since the inductor  $L$  releases energy quickly, the voltage falls back to a value equal to  $V_{pv}$  when the inductor  $L$  has no more stored energy to release. These statements fully explain how a boost converter increase the voltage supplied to the load  $R$  (end-user) by acting like a voltage regulator [173,174].

For ease of reference, Figure 13a shows the circuit layout of the converter when the MOSFET is switched “OFF”, and Figure 13b shows the circuit layout of the converter when the MOSFET is switched “ON”. As prior knowledge,  $I_{pv}$  and  $V_{pv}$  correspond to the variables on the  $I$ - $V$  characteristic curve of the PV panel. As we expand on the explanation, when the MOSFET is switched “ON” to create a short circuit path with negligible resistance,  $I_{pv}$  begins to rise to  $I_{sc}$  and  $V_{pv}$  starts to drop to zero. Conversely, when the MOSFET is switched “OFF” to create an open circuit path with infinite resistance,  $I_{pv}$  begins to drop to zero and  $V_{pv}$  starts to rise to  $V_{oc}$ . Hence, the ratio of the “ON” to “OFF” intervals of the MOSFET over a period of time regulates the amount of current and voltage that can be extracted from the PV panel. In fact, a PWM signal  $S$  that turns the MOSFET “ON” or “OFF” at high frequency reduces oscillations for effective stabilization.

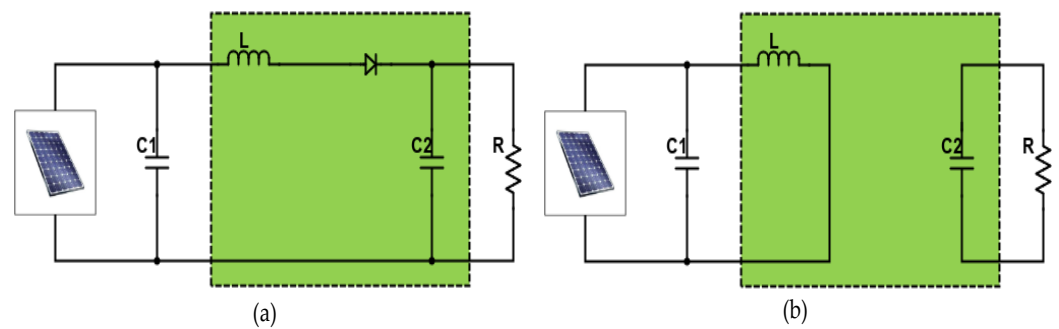


Figure 13. Circuit layout when MOSFET is (a) toggled ON or (b) toggled OFF.

Instead, we can also summarize the architecture from other perspectives [174]:

- (1) The digital PWM signal  $S$  contributes to the “ON” to “OFF” ratio of the MOSFET for duration within a period.
- (2) As the inductor  $L$  releases energy when the MOSFET is turned “OFF”, the sign of the inductor  $L$  is reversed, the positive sign of the PV panel is connected to the negative sign of the inductor  $L$ , and the total voltage received by the load  $R$  is now an added value. Therefore, it can be reasonably deduced that  $\max(V_{pv}) \leq \max(V_R)$ .
- (3) The power drawn from the PV panel should theoretically be equivalent to the power delivered to the load  $R$  due to the effective voltage stabilization when the MOSFET is switched “ON” and “OFF” at fixed time intervals during high frequency cycles. Hence,  $P_R \approx P_{pv}$ .
- (4) As  $P_R \approx P_{pv}$  and  $\max(V_{pv}) \leq \max(V_R)$ , the current drawn from the PV panel is theoretically larger than the current supplied to the load, and, hence,  $\max(I_{pv}) \geq \max(I_R)$ .

Throughout evolution, a large number of improved ideas and setups for DC–DC boost converters have been proposed with the aim of increasing the efficiency of circuit (energy) conversion in PV systems. The following literatures [175–179] are cited for further investigation.

## 5.2. Converter Topologies

At the current stage, conventional DC–DC boost converter topologies have reached their limits and cannot continue to achieve the desired voltage gain levels without subjecting the power semiconductor components to extremely high duty cycle and voltage stress. For further breakthroughs, many researchers have extended beyond the conventional boost converter

topology to achieve higher voltage gain with greater efficiency and reliability [180–182]. As outcomes, DC–DC boost converters can now be further classified into numerous topologies. Upon research studies, this review article examines five topologies branching off from the HGLP DC–DC boost converters that have lately drawn a lot of interest: cascading techniques, voltage multiplier cells (VMC) or voltage doubler, voltage lift techniques, multi-phase, and transformer-less. Table 10 collects numerous novel boost converter models that fall into these topologies and provides a comprehensive comparison based on released year, tested frequency, voltage gain, and peak efficiency. About 30 references from 2020 to 2022 are cited in Table 10 to support an in-depth discussion. It basically shows the hierarchical evolution of various HGLP boost converter topologies, that have recently been popularized by researchers over the past 2 years.

**Table 10.** Hierarchical evolution of various HGLP boost converter topologies (2020–2022).

Topology	Ref.	Year of Proposal	Tested Frequency (kHz)	Voltage Gain ( $\times$ )	Peak Efficiency (%)
Cascading techniques	[183]	2020	50	12.00	93.00
	[184]	2021	10	10.00	NA
	[185]	2021	20	10.42	87.00
	[186]	2021	100	7.00	91.15
	[187]	2022	22	1.90	90.00
	[188]	2022	50	7.92	95.23
Voltage multiplier cells (VMC) or voltage doubler	[189]	2020	118	25.00	96.70
	[190]	2021	10	13.33	NA
	[191]	2021	NA	10.00	90.00
	[192]	2022	20	10.00	90.00
	[193]	2022	100	11.52	91.60
	[194]	2022	100	9.50	97.23
	[195]	2022	40	10.00	97.44
	[196]	2022	90	16.67	97.50
Voltage lift techniques	[197]	2020	50	12.00	96.00
	[198]	2021	50	7.10	95.70
	[193]	2022	100	11.52	91.60
	[199]	2022	50	16.67	94.50
	[200]	2022	50	14.95	95.80
Multi-phase boost converter	[197]	2020	50	12.00	96.00
	[201]	2021	25	15.00	93.00
	[202]	2021	350	4.00	98.30
	[203]	2022	50	2.23	94.00
	[204]	2022	5	2.19	95.74
	[205]	2022	30	10.00	98.68

Table 10. Cont.

Topology	Ref.	Year of Proposal	Tested Frequency (kHz)	Voltage Gain ( $\times$ )	Peak Efficiency (%)
Transformer-less boost converter	[206]	2020	50	10.00	95.30
	[207]	2021	10	11.25	90.00
	[208]	2021	100	10.00	92.43
	[209]	2021	20	10.00	95.00
	[210]	2021	50	6.67	95.44
	[211]	2022	40	2.47	97.40
	[212]	2022	30	10.00	88.00

From research analysis, it is difficult to define which topology has the best converter performance, as each topology has its own model that successfully achieves a voltage gain above 10.00 and a peak efficiency greater than 95.00%. Several DC–DC converter topologies that inherit high voltage gain capability are reviewed. However, these converters are under too much voltage stress to raise the voltage from a very small supply [213]. Meanwhile, the efficiency of some of these converters will drop sharply if the voltage conversion ratio is too high. Hence, in addition to minimizing current-ripple and preventing the converter from running at extreme duty frequency, it is worth noting that high-voltage stress on the switches is a major concern for high-gain DC–DC boost converters [214]. The challenge for DC–DC boost converters remains to maximize voltage gain while maintaining maximum efficiency. It is always the goal to achieve a high-voltage gain DC–DC boost converter with higher power-handling capability, high efficiency and higher power density at low cost [162].

## 6. Conclusions

All these research findings will help readers understand the architecture of PV systems, thereby making it easier for them to build, model and simulate MPPT applications for photovoltaic systems. We have presented all the relevant knowledge regarding the complete mechanism of photovoltaic (PV) systems. PV systems demand high voltages for efficient transmission through power transmission systems. The PV system is mainly composed of a PV panel, controller and boost converter. Each electro-device plays its own role in the entire PV power generation system.

The PV panel is the power-generating device, where all power-generating processes are initiated. It is basically regarded as a PV array with multiple modules connected in parallel and in series. However, the PV module is not the smallest compound in PV panel, the PV cell is. Multiple PV cells are connected in series to establish a PV module, and PV cells are the real compounds responsible for generating PV power based on operating irradiance and ambient temperature. Researchers have been working on developing innovative PV solar cells through continuous distribution, modification, reconfiguration, combination, dosage and other chemical manipulations. Up until now, photovoltaic solar cell companions have evolved through four generations. From the discussion, we inferred that the fourth-generation solar cells will continue to maintain strong growth expectations in the future, and they are expected to occupy half of the research market in the next few years. The only challenge lies in determining the proportional concentration of nanomaterials used in the solar cell. Improper rationing can lead to defects that instead assimilate light from the solar cells, reducing the energy conversion efficiency of the solar cell.

In a PV module, the open-circuit voltage ( $V_{oc}$ ), short-circuit current ( $I_{sc}$ ) and power at MPP ( $P_{mp}$ ) decrease with increasing shading. The PV array (panel) produces a more complex shape on the  $P$ - $V$  characteristic curve when PV modules are interconnected in series under partially shaded conditions. To overcome the power loss mismatch caused

by partial shading, researchers have been exploiting the potential of various PV array configurations to achieve more stable, robust and efficient power generation from PV panels. This article reviewed five PV array configurations: series, series-parallel, honeycomb, bridge-link, and tripled-tied. Based on the analysis of the collected data, it was inferred that the tripled-tied configuration has the best performance and stability, which is probably the best solution against the impacts of partial shading conditions. However, from an in-depth discussion, it was concluded that research on PV array configurations has reached certain limitations. Further development of PV array configurations is expected to slow down in the coming years, while the challenge remains that of how to efficiently and sustainably harvest maximum power with small relative errors under load-bearing environmental conditions.

The controller is an electronic device that controls the circulating circuits in a PV system to collect as much power as possible from the solar panel. It basically consists of a maximum power point tracking (MPPT) module and a PWM generator. The MPPT module installs MPPT technique to optimize certain vital parameters, while referencing PV panel data and environmental data for any better duty cycle solution. The PWM generator then receives the tuned duty cycle (varies from 0 to 1) to create the desired structure (successive “ON” to “OFF” ratio per period time) in the controlling signal to be sent to the boost converter. MPPT techniques have continued to develop over the years. This paper reviewed 20 novel MPPT techniques proposed from 2019 to 2022, all of which are categorized as any of classical, smart, optimized, and hybrid MPPTs. Throughout the course of the inquiry, we discovered that numerous novel MPPT techniques inspired by various intelligent approaches and metaheuristic optimization algorithms provide more efficient solutions than existing traditional MPPT techniques. Obviously, from 2021, researchers have started to switch the concern of the development to the optimization MPPT techniques. All combined facts indicate that the optimization MPPT techniques can currently be the best compatible to the photovoltaic applications. In-depth research on optimization MPPT is expected to be a near-term trend, at least in the future 5 years.

A DC–DC boost converter is typically adopted by a PV system in the process. It acts as a voltage regulator to stabilize the PV output while specifically amplifying the PV voltage to be sent to the load user. Through research, we knew that this boost converter is more like a centroid device, which receives instructions from the controller via a pulse wave modulation (PWM) signal, and then systematically extracts a specified amount of PV output from the PV panel. If PWM signal sends an “ON” signal, the MOSFET is toggled “ON”, otherwise the MOSFET is toggled “OFF”. Overall, all processes in the boost converter are reasonably controlled by the controller. From other perspectives of verification, we also defined that the PV voltage must be less than the voltage at load, the PV power ought to be roughly equivalent to the power at load, and the PV current must be larger than the current at load. For further breakthroughs on converter technology, many researchers have extended beyond the conventional boost converter topology to achieve higher voltage gain with greater efficiency and reliability. This article reviewed around 30 novel boost converter models (from 2020 to 2022) classified into five topologies (i.e., cascading techniques, voltage multiplier cells (VMC) or voltage doublers, voltage lift techniques, multi-phase, and transformer-less) and provides a comprehensive comparison based on released year, tested frequency, voltage gain, and peak efficiency. From research analysis, it was difficult to define which topology has the best converter performance, as each topology has its own model that successfully achieves a voltage gain above 10.00 and a peak efficiency greater than 95.00%. The challenge for DC–DC boost converters remains to maximize voltage gain while maintaining maximum efficiency with higher power handling capability, high efficiency and higher power density at low cost.

**Author Contributions:** Conceptualization, W.-H.T. and J.M.-S.; methodology, W.-H.T.; software, W.-H.T.; validation, W.-H.T. and J.M.-S.; formal analysis, W.-H.T.; investigation, W.-H.T.; resources, W.-H.T.; data curation, W.-H.T.; writing—original draft preparation, W.-H.T.; writing—review and editing, W.-H.T.; visualization, W.-H.T.; supervision, J.M.-S.; project administration, J.M.-S.; funding acquisition, J.M.-S. All authors have read and agreed to the published version of the manuscript.

**Funding:** This research was funded by the Fundamental Research Grant Scheme of the Ministry of Higher Education (MOHE) of Malaysia, grant number FRGS/1/2021/TK0/USM/02/14.

**Institutional Review Board Statement:** Not applicable.

**Informed Consent Statement:** Not applicable.

**Data Availability Statement:** Not applicable.

**Acknowledgments:** The Fundamental Research Grant Scheme of the Ministry of Higher Education (MOHE) of Malaysia provided funding for this study (Grant No. FRGS/1/2021/TK0/USM/02/14).

**Conflicts of Interest:** The authors declare no conflict of interest. The funders had no role in the design of the study; in the collection, analyses, or interpretation of data; in the writing of the manuscript; or in the decision to publish the results.

## References

1. Rio, J.; Silitonga, P. *Energy Efficiency Cambodia Promoting and Demonstrating Energy Management System in Cambodia*; ASEAN Centre of Energy: Jakarta, Indonesia, 2020.
2. Tao, M.; Hamada, H.; Druffel, T.; Lee, J.-J.; Rajeshwar, K. Review—Research Needs for Photovoltaics in the 21st Century. *ECS J. Solid State Sci. Technol.* **2020**, *9*, 125010. [[CrossRef](#)]
3. Mao, M.; Duan, Q.; Duan, P.; Hu, B. Comprehensive improvement of artificial fish swarm algorithm for global MPPT in PV system under partial shading conditions. *Trans. Inst. Meas. Control.* **2018**, *40*, 2178–2199. [[CrossRef](#)]
4. Wang, W.; Yu, N.; Johnson, R. A model for commercial adoption of photovoltaic systems in California. *J. Renew. Sustain. Energy* **2017**, *9*, 025904. [[CrossRef](#)]
5. Wei, C.K.; Saad, A.Y. The Potential of Solar Energy for Domestic and Commercial Buildings in Malaysia. *J. Adv. Res. Fluid Mech. Therm. Sci.* **2020**, *75*, 91–98. [[CrossRef](#)]
6. Nwaigwe, K.N.; Mutabilwa, P.; Dintwa, E. An overview of solar power (PV systems) integration into electricity grids. *Mater. Sci. Energy Technol.* **2019**, *2*, 629–633. [[CrossRef](#)]
7. Ceran, B.; Jurasz, J.; Mielcarek, A.; Campana, P.E. PV systems integrated with commercial buildings for local and national peak load shaving in Poland. *J. Clean. Prod.* **2021**, *322*, 129076. [[CrossRef](#)]
8. Ontiri, G.K.; Amuhaya, L.L. A Review of Emerging Photovoltaic Construction Technologies to Increase Efficiencies in Solar as a Renewable Energy Source. *Am. Acad. Sci. Res. J. Eng. Technol. Sci.* **2022**, *85*, 348–369.
9. Kumari, J.S.; Babu, C.S. Mathematical Modeling and Simulation of Photovoltaic Cell using Matlab-Simulink Environment. *Int. J. Electr. Comput. Eng.* **2015**, *2*, 26–34. [[CrossRef](#)]
10. Seyedmahmoudian, M.; Mekhilef, S.; Rahmani, R.; Yusof, R.; Renani, E.T. Analytical Modeling of Partially Shaded Photovoltaic Systems. *Energies* **2013**, *6*, 128–144. [[CrossRef](#)]
11. Sathyanarayana, P.; Ballal, R.; Sagar, P.L.; Kumar, G. Effect of Shading on the Performance of Solar PV Panel. *Energy Power* **2015**, *5*, 1–4. [[CrossRef](#)]
12. Babu, G.S.; Charan, B.P.; Krishna, A.R. Comparative analysis of I-V & P-V characteristics of a series and parallel connected SPV modules. *Int. J. Curr. Eng. Sci. Res. (IJCESR)* **2016**, *3*, 1–6.
13. Tiwari, G.N.; Meraj, M.; Khan, M.E.; Dwevedi, V.K. Effect of Series and Parallel Combination of Photovoltaic Thermal Collectors on the Performances of Integrated Active Solar Still. *J. Therm. Sci. Eng. Appl.* **2022**, *14*, 081006. [[CrossRef](#)]
14. Gallegos, C.D.R.; Alvarez-Alvarado, M.S. Analysis of the Stationary and Transient Behavior of a Photovoltaic Solar Array: Modeling and Simulation. *Int. J. Comput. Appl. Technol.* **2015**, *127*, 26–33. [[CrossRef](#)]
15. Parthiban, R.; Ponnambalam, P. An Enhancement of the Solar Panel Efficiency: A Comprehensive Review. *Front. Energy Res.* **2022**, *10*, 937155. [[CrossRef](#)]
16. Salem, F.; Awadallah, M.A. Detection and assessment of partial shading in photovoltaic arrays. *J. Electr. Syst. Inf. Technol.* **2016**, *3*, 23–32. [[CrossRef](#)]
17. Saadsaoud, M.; Abbassi, H.A.; Kermiche, S.; Ouada, M. Study of Partial Shading Effects on Photovoltaic Arrays with Comprehensive Simulator for Global MPPT Control. *Int. J. Renew. Energy Res.* **2016**, *6*, 413–420.
18. Dadjé, A.; Djongyang, N.; Tchinda, R. Electrical Power Losses in a Photovoltaic Solar Cell Operating under Partial Shading Conditions. *J. Power Energy Eng.* **2017**, *5*, 19–33. [[CrossRef](#)]
19. Soomar, A.M.; Hakeem, A.; Messaoudi, M.; Musznicki, P.; Iqbal, A.; Czapp, S. Solar Photovoltaic Energy Optimization and Challenges. *Front. Energy Res.* **2022**, *10*, 1–18. [[CrossRef](#)]
20. Tofoli, F.L.; de Pereira, D.C.; de Paula, W.J. Comparative Study of Maximum Power Point Tracking Techniques for Photovoltaic Systems. *Int. J. Photoenergy* **2015**, *2015*, 1–10. [[CrossRef](#)]
21. Pakkiraiah, B.; Sukumar, G.D. Research Survey on Various MPPT Performance Issues to Improve the Solar PV System Efficiency. *J. Sol. Energy* **2016**, *2016*, 1–20. [[CrossRef](#)]
22. Lu, Y.; Khan, Z.A.; Alvarez-Alvarado, M.S.; Zhang, Y.; Huang, Z.; Imran, M. A Critical Review of Sustainable Energy Policies for the Promotion of Renewable Energy Sources. *Sustainability* **2020**, *12*, 5078. [[CrossRef](#)]

23. ASEAN. *ASEAN Action Plan for Energy Cooperation (APAEC) 2016–2025*; Zamora, C.G., Ed.; ASEAN Centre for Energy: Jakarta, Indonesia, 2015.
24. Dewangan, D.; Ekka, J.P.; Arjunan, T.V. Solar photovoltaic thermal system: A comprehensive review on recent design and development, applications and future prospects in research. *Int. J. Ambient Energy* **2022**, *43*, 1–25. [[CrossRef](#)]
25. Decker, C. Energy transportation: Electricity. In *Handbook of Energy Economics and Policy—Fundamentals and Applications for Engineers and Energy Planners*; Rubino, A., Sapio, A., Scala, M.L., Eds.; Academic Press: Cambridge, MA, USA, 2021; pp. 193–238. ISBN 978-0-12-814712-2.
26. Paynter, R.T.; Boydell, B.J.T. Power Transmission and Distribution: An Overview. In *Introduction to Electricity*; Pearson: Upper Saddle River, NJ, USA, 2010; pp. 1095–1097.
27. Annestrand, S.A. Power Transmission, High-Voltage. In *Encyclopedia of Physical Science and Technology*; Academic Press: Cambridge, MA, USA, 2003; pp. 35–55. [[CrossRef](#)]
28. Paynter, R.T.; Boydell, B.J.T. Transmission Lines and Substations. In *Introduction to Electricity*; Pearson: Upper Saddle River, NJ, USA, 2010; pp. 1102–1104.
29. Dhass, A.D.; Beemkumar, N.; Harikrishnan, S.; Ali, H.M. A Review on Factors Influencing the Mismatch Losses in Solar Photovoltaic System. *Int. J. Photoenergy* **2022**, 1–27. [[CrossRef](#)]
30. Engr Alumona, T.L.; Nwosu, M.O.; Ezechukwu, A.O.; Chijioko, J. Overview Of Losses And Solutions In Power Transmission Lines. *Netw. Complex Syst.* **2014**, *4*, 24–31.
31. Doukas, H.; Karakosta, C.; Flamos, A.; Psarras, J. Electric power transmission: An overview of associated burdens. *Int. J. Energy Res.* **2011**, *35*, 979–988. [[CrossRef](#)]
32. Hameiri, Z. Photovoltaics literature survey (no. 172). *Prog. Photovolt.* **2022**, *30*, 204–208. [[CrossRef](#)]
33. Sarah, K.E.; Roland, U.; Ci, O.E.N. A Review of Solar Photovoltaic Technologies. *Int. J. Eng. Res. Technol.* **2020**, *9*, 741–749. [[CrossRef](#)]
34. IEA. *Renewables 2021: Analysis and Forecasts to 2026*; OECD Publishing: Paris, France, 2021.
35. Sedra, A.S.; Smith, K.C. *Microelectronic Circuits 5TH Edition*; Oxford University Press: Oxford, UK, 2004; ISBN 0195142527.
36. Dambhare, M.V.; Butey, B.; Moharil, S. V Solar photovoltaic technology: A review of different types of solar cells and its future trends. *J. Phys. Conf. Ser.* **2021**, *1913*, 1–16. [[CrossRef](#)]
37. Moller, H.J. *Semiconductors for Solar Cells*; Artech House: Norwood, MA, USA, 1993; ISBN 9780890065747.
38. Fahrenbruch, A.; Bube, R. *Fundamentals Of Solar Cells*; Academic Press: Cambridge, MA, USA, 1983; ISBN 9780323145381.
39. Villalva, M.G.; Gazoli, J.R.; Filho, E.R. Comprehensive Approach to Modeling and Simulation of Photovoltaic Arrays. *IEEE Trans. Power Electron.* **2009**, *24*, 1198–1208. [[CrossRef](#)]
40. Salmi, T.; Bouzguenda, M.; Gastli, A.; Masmoudi, A. MATLAB/Simulink Based Modelling of Solar Photovoltaic Cell. *Int. J. Renew. Energy Res.* **2012**, *2*, 213–218.
41. Hossain, M.S.; Roy, N.K.; Ali, M.O. Modeling of solar photovoltaic system using MATLAB/Simulink. In Proceedings of the 2016 19th International Conference on Computer and Information Technology (ICCIT), Dhaka, Bangladesh, 18–20 December 2016; p. 16692888.
42. Vergura, S. A Complete and Simplified Datasheet-Based Model of PV Cells in Variable Environmental Conditions for Circuit Simulation. *Energies* **2016**, *9*, 326. [[CrossRef](#)]
43. Kesİlmİş, Z.; Erol, H.; Uçman, M. Power Optimization in Partially Shaded Photovoltaic Systems. *Tech. J.* **2018**, *12*, 34–38. [[CrossRef](#)]
44. De Soto, W.; Klein, S.A.; Beckman, W.A. Improvement and validation of a model for photovoltaic array performance. *Sol. Energy* **2006**, *80*, 78–88. [[CrossRef](#)]
45. Jahangir, A.; Mishra, S. Autonomous Battery Storage Energy System Control of PV-Wind Based DC Microgrid. In Proceedings of the 2018 2nd International Conference on Power, Energy and Environment: Towards Smart Technology (ICEPE), Shillong, India, 1–2 June 2018; p. 18508739.
46. Messenger, R.A.; Abtahi, A. *Photovoltaic Systems Engineering*, 4th ed.; CRC Press: Boca Raton, FL, USA, 2017; ISBN 9781498772778.
47. Prakash, R.; Singh, S. Designing and Modelling of Solar Photovoltaic Cell and Array. *IOSR J. Electr. Electron. Eng.* **2016**, *11*, 35–40. [[CrossRef](#)]
48. Rauschenbach, H.S. *Solar Cell Array Design Handbook: The Principles and Technology of Photovoltaic Energy Conversion*; Springer: Dordrecht, The Netherlands, 1980; Volume 1. [[CrossRef](#)]
49. Seyedmahmoudian, M.; Mohamadi, A.; Kumary, S.; Maung, A.; Oo, T.; Stojcevski, A. A Comparative Study on Procedure and State of the Art of Conventional Maximum Power Point Tracking Techniques for Photovoltaic System. *Int. J. Comput. Electr. Eng.* **2014**, *6*, 402–414. [[CrossRef](#)]
50. Pastuszak, J.; Wegierek, P. Photovoltaic Cell Generations and Current Research Directions for Their Development. *Materials* **2022**, *15*, 5542. [[CrossRef](#)]
51. Kuczyńska-Łażewska, A.; Klugmann-Radziemska, E.; Witkowska, A. Recovery of Valuable Materials and Methods for Their Management When Recycling Thin-Film CdTe Photovoltaic Modules. *Materials* **2021**, *14*, 7836. [[CrossRef](#)] [[PubMed](#)]
52. Al-Ezzi, A.S.; Ansari, M.N.M. Photovoltaic Solar Cells: A Review. *Appl. Syst. Innov.* **2022**, *5*, 67. [[CrossRef](#)]
53. Rathore, N.; Panwar, N.L.; Yettou, F.; Gama, A. A comprehensive review of different types of solar photovoltaic cells and their applications. *Int. J. Ambient Energy* **2021**, *42*, 1200–1217. [[CrossRef](#)]

54. Iqbal, M.A.; Malik, M.; Shahid, W.; Din, S.Z.U.; Anwar, N.; Ikram, M.; Idrees, F. Materials for Photovoltaics: Overview, Generations, Recent Advancements and Future Prospects. In *Thin Films Photovoltaics*; Zaidi, B., Shekhar, C., Eds.; IntechOpen: London, UK, 2022; pp. 1–112.
55. Best Research-Cell Efficiency Chart. NREL Transforming ENERGY. 2022. Available online: <https://www.nrel.gov/pv/cell-efficiency.html> (accessed on 21 November 2022).
56. Čulík, P.; Brooks, K.; Momblona, C.; Adams, M.; Kinge, S.; Maréchal, F.; Dyson, P.J.; Nazeeruddin, M.K. Design and Cost Analysis of 100 MW Perovskite Solar Panel Manufacturing Process in Different Locations. *ACS Energy Lett.* **2022**, *7*, 3039–3044. [[CrossRef](#)]
57. Muteri, V.; Cellura; Curto, D.; Franzitta; Longo, S.; Mistretta; Parisi, M.L. Review on Life Cycle Assessment of Solar Photovoltaic Panels. *Energies* **2020**, *13*, 252. [[CrossRef](#)]
58. Fthenakis, V.M.; Kim, H.C. Photovoltaics: Life-cycle analyses. *Sol. Energy* **2011**, *85*, 1609–1628. [[CrossRef](#)]
59. Sopian, K.; Cheow, S.L.; Zaidi, S.H. An overview of crystalline silicon solar cell technology: Past, present, and future. *AIP Conf. Proc.* **2017**, *1877*, 020004. [[CrossRef](#)]
60. Jones, C.; Gilbert, P. Determining the consequential life cycle greenhouse gas emissions of increased rooftop photovoltaic deployment. *J. Clean. Prod.* **2018**, *184*, 211–219. [[CrossRef](#)]
61. Fathi, M.; Mefoued, A.; Messaoud, A.; Boukennou, Y. Cost-effective photovoltaics with silicon material. *Phys. Procedia* **2009**, *2*, 751–757. [[CrossRef](#)]
62. Hengevoss, D.; Baumgartner, C.; Nisato, G.; Hugli, C. Life Cycle Assessment and eco-efficiency of prospective, flexible, tandem organic photovoltaic module. *Sol. Energy* **2016**, *137*, 317–327. [[CrossRef](#)]
63. Louwen, A.; Van-Sark, W.; Schropp, R.; Faaij, A. A cost roadmap for silicon heterojunction solar cells. *Sol. Energy Mater. Sol. Cells* **2016**, *147*, 295–314. [[CrossRef](#)]
64. Tian, X.; Stranks, S.D.; You, F. Life cycle energy use and environmental implications of high-performance perovskite tandem solar cells. *Sci. Adv.* **2020**, *6*, 1–10. [[CrossRef](#)] [[PubMed](#)]
65. Jean, J.; Brown, P.R.; Jaffe, R.L.; Buonassisi, T.; Bulović, V. Pathways for solar photovoltaics. *Energy Environ. Sci.* **2015**, *8*, 1200–1219. [[CrossRef](#)]
66. Resalati, S.; Okoroafor, T.; Maalouf, A.; Saucedo, E.; Placidi, M. Life cycle assessment of different chalcogenide thin-film solar cells. *Appl. Energy* **2022**, *313*, 118888. [[CrossRef](#)]
67. Horowitz, K.A.W.; Woodhouse, M. Cost and potential of monolithic CIGS photovoltaic modules. In Proceedings of the 2015 IEEE 42nd Photovoltaic Specialist Conference (PVSC), New Orleans, LA, USA, 14–19 June 2015; p. 15664730.
68. Rix, A.; Steyl, J.; Rudman, J.; Terblanche, U.; Van-Niekerk, J. *First Solar's CdTe Module Technology—Performance, Life Cycle, Health and Safety Impact Assessment*; Centre for Renewable and Sustainable Energy Studies, Stellenbosch University: Stellenbosch, South Africa, 2015.
69. Kim, H.C.; Fthenakis, V.; Choi, J.-K.; Turney, D.E. Life Cycle Greenhouse Gas Emissions of Thin-film Photovoltaic Electricity Generation. *J. Ind. Ecol.* **2012**, *16*, S110–S121. [[CrossRef](#)]
70. Águas, H.; Ram, S.K.; Araújo, A.J.; Gaspar, D.; Vicente, A.M.T.; Filonovich, S.; Fortunato, E.; Martins, R.F.; Ferreira, I. Silicon thin film solar cells on commercial tiles. *Energy Environ. Sci.* **2011**, *4*, 4620–4632. [[CrossRef](#)]
71. Rao, V.T.; Sekhar, Y.R.; Mahesh, H.; Muraleedharan, A.K.; Charles, D.; Aljuraide, N.I.; Ibrahim, A.M.M.; Helal, M.; Galal, A.M.; Sami, R.; et al. Life Cycle Analysis of Thin-Film Photovoltaic Thermal Systems for Different Tropical Regions. *Sustainability* **2022**, *14*, 14209. [[CrossRef](#)]
72. Chen, Y.; Altermatt, P.P.; Chen, D.; Zhang, X.; Xu, G.; Yang, Y.; Wang, Y.; Feng, Z.; Shen, H.; Verlinden, P.J. From Laboratory to Production: Learning Models of Efficiency and Manufacturing Cost of Industrial Crystalline Silicon and Thin-Film Photovoltaic Technologies. *IEEE J. Photovoltaics* **2018**, *8*, 1531–1538. [[CrossRef](#)]
73. Horowitz, K.A.; Remo, T.W.; Smith, B.; Ptak, A.J. *A Techno-Economic Analysis and Cost Reduction Roadmap for III-V Solar Cells*; National Renewable Energy Lab. (NREL): Golden, CO, USA, 2018.
74. Lee, K.; Lee, J.; Mazor, B.A.; Forrest, S.R. Transforming the cost of solar-to-electrical energy conversion: Integrating thin-film GaAs solar cells with non-tracking mini-concentrators. *Light Sci. Appl.* **2015**, *4*, e288. [[CrossRef](#)]
75. Kalowekamo, J.; Baker, E. Estimating the manufacturing cost of purely organic solar cells. *Sol. Energy* **2009**, *83*, 1224–1231. [[CrossRef](#)]
76. Tsang, M.P.; Sonnemann, G.W.; Bassani, D.M. Life-cycle assessment of cradle-to-grave opportunities and environmental impacts of organic photovoltaic solar panels compared to conventional technologies. *Sol. Energy Mater. Sol. Cells* **2016**, *156*, 37–48. [[CrossRef](#)]
77. Espinosa, N.; Krebs, F.C. Life cycle analysis of organic tandem solar cells: When are they warranted? *Sol. Energy Mater. Sol. Cells* **2014**, *120*, 692–700. [[CrossRef](#)]
78. Jean, J.; Xiao, J.; Nick, R.; Moody, N.; Nasilowski, M.; Bawendi, M.; Bulović, V. Synthesis cost dictates the commercial viability of lead sulfide and perovskite quantum dot photovoltaics. *Energy Environ. Sci.* **2018**, *11*, 2295–2305. [[CrossRef](#)]
79. Schoden, F.; Schnatmann, A.K.; Blachowicz, T.; Manz-Schumacher, H.; Schwenzfeier-Hellkamp, E. Circular Design Principles Applied on Dye-Sensitized Solar Cells. *Sustainability* **2022**, *14*, 15280. [[CrossRef](#)]
80. Li, Z.; Zhao, Y.; Wang, X.; Sun, Y.; Zhao, Z.; Li, Y.; Zhou, H.; Chen, Q. Cost Analysis of Perovskite Tandem Photovoltaics. *Joule* **2018**, *2*, 1559–1572. [[CrossRef](#)]

81. Ahangharnejhad, R.H.; Phillips, A.B.; Song, Z.; Celik, I.; Ghimire, K.; Koirala, P.; Ellingson, R.J.; Collins, R.W.; Podraza, N.J.; Yan, Y.; et al. Impact of lifetime on the levelized cost of electricity from perovskite single junction and tandem solar cells. *Sustain. Energy Fuels* **2022**, *6*, 2718–2726. [[CrossRef](#)]
82. Syed, T.H.; Wei, W. Technoeconomic Analysis of Dye Sensitized Solar Cells (DSSCs) with WS<sub>2</sub>/Carbon Composite as Counter Electrode Material. *Inorganics* **2022**, *10*, 191. [[CrossRef](#)]
83. Zendejdel, M.; Nia, N.Y.; Yaghoubinia, M. *Emerging Thin Film Solar Panels. In Reliability and Ecological Aspects of Photovoltaic Modules*; InTechOpen: London, UK, 2019; pp. 1–26. [[CrossRef](#)]
84. Baiju, A.; Yarema, M. Status and challenges of multi-junction solar cell technology. *Front. Energy Res.* **2022**, *10*, 1–17. [[CrossRef](#)]
85. Itten, R.; Stucki, M. Highly Efficient 3rd Generation Multi-Junction Solar Cells Using Silicon Heterojunction and Perovskite Tandem: Prospective Life Cycle Environmental Impacts. *Energies* **2017**, *10*, 841. [[CrossRef](#)]
86. Horowitz, K.; Woodhouse, M.; Lee, H.; Smestad, G. A Bottom-Up Cost Analysis of a High Concentration PV Module. *AIP Conf. Proc.* **2015**, *1679*, 100001. [[CrossRef](#)]
87. Gao, Q.; Yan, J.; Wan, L.; Zhang, C.; Wen, Z.; Zhou, X.; Li, H.; Li, F.; Chen, J.; Guo, J.; et al. High-Efficiency Graphene-Oxide/Silicon Solar Cells with an Organic-Passivated Interface. *Adv. Mater. Interfaces* **2022**, *9*, 2201221. [[CrossRef](#)]
88. Jang, C.W.; Shin, D.H.; Choi, S.-H. Porous silicon solar cells with 13.66% efficiency achieved by employing graphene-quantum-dots interfacial layer, doped-graphene electrode, and bathocuproine back-surface passivation layer. *J. Alloys Compd.* **2021**, *877*, 160311. [[CrossRef](#)]
89. Hong, J.A.; Jung, E.D.; Yu, J.C.; Kim, D.W.; Nam, Y.S.; Oh, I.; Lee, E.; Yoo, J.-W.; Cho, S.; Song, M.H. Improved Efficiency of Perovskite Solar Cells Using a Nitrogen-Doped Graphene-Oxide-Treated Tin Oxide Layer. *ACS Appl. Mater. Interfaces* **2020**, *12*, 2417–2423. [[CrossRef](#)]
90. Zhang, S.; Guo, R.; Zeng, H.; Zhao, Y.; Liu, X.; You, S.; Li, M.; Luo, L.; Lira-Cantu, M.; Li, L.; et al. Improved performance and stability of perovskite solar modules by interface modulating with graphene oxide crosslinked CsPbBr<sub>3</sub> quantum dots. *Energy Environ. Sci.* **2022**, *15*, 244–253. [[CrossRef](#)]
91. Nagaraj, G.; Mohammed, M.K.A.; Shekargoftar, M.; Sasikumar, P.; Sakthivel, P.; Ravi, G.; Dehghanipour, M.; Akin, S.; Shalan, A.E. High-performance perovskite solar cells using the graphene quantum dot–modified SnO<sub>2</sub>/ZnO photoelectrode. *Mater. Today Energy* **2021**, *22*, 100853. [[CrossRef](#)]
92. Mahalingam, S.; Low, F.W.; Omar, A.; Manap, A.; Rahim, N.A.; Tan, C.H.; Abdullah, H.; Voon, C.H.; Rokhmat, M.; Wibowo, E.; et al. Zinc oxide/graphene nanocomposite as efficient photoelectrode in dye-sensitized solar cells: Recent advances and future outlook. *Int. J. Energy Res.* **2022**, *46*, 7082–7100. [[CrossRef](#)]
93. Huang, X.; Hara, E.; Sugime, H.; Noda, S. Carbon nanotube/silicon heterojunction solar cell with an active area of 4 cm<sup>2</sup> realized using a multifunctional molybdenum oxide layer. *Carbon N. Y.* **2021**, *185*, 215–223. [[CrossRef](#)]
94. Tazawa, Y.; Habisreutinger, S.N.; Zhang, N.; Gregory, D.A.F.; Nagamine, G.; Kesava, S.V.; Mazzotta, G.; Assender, H.E.; Riede, M.; Padilha, L.A.; et al. Carbon Nanotubes for Quantum Dot Photovoltaics with Enhanced Light Management and Charge Transport. *ACS Photonics* **2018**, *5*, 4854–4863. [[CrossRef](#)]
95. Mfon, R.E.; Labulo, A.H.; Al Amri, Z.; Esaduwha, S.; Labaran, J. Effect of Carbon Nanotubes on the performance of Perovskite Solar Cells. *Eur. J. Energy Res.* **2022**, *2*, 62–68. [[CrossRef](#)]
96. Shao, W.; Wu, W. High-Efficiency (Over 10%) Parallel Tandem Dye-Sensitized Solar Cells Based on Tri-Carbon Electrodes. *Trans. Tianjin Univ.* **2022**, *28*, 414–422. [[CrossRef](#)]
97. Hu, X.-G.; Wei, Q.; Zhao, Y.-M.; Hou, P.-X.; Ren, W.; Liu, C.; Cheng, H.-M. FeCl<sub>3</sub>-functionalized graphene oxide/single-wall carbon nanotube/silicon heterojunction solar cells with an efficiency of 17.5%. *J. Mater. Chem. A* **2022**, *10*, 4644–4652. [[CrossRef](#)]
98. Gopi, C.V.V.M.; Singh, S.; Reddy, A.E.; Kim, H.-J. CNT@rGO@MoCuSe Composite as an Efficient Counter Electrode for Quantum Dot-Sensitized Solar Cells. *ACS Appl. Mater. Interfaces* **2018**, *10*, 10036–10042. [[CrossRef](#)] [[PubMed](#)]
99. Zhao, X.; Wu, Y.; Xia, Z.; Chang, S.; Shang, Y.; Cao, A. A GQD-based composite film as photon down-converter in CNT/Si solar cells. *Nano Res.* **2021**, *14*, 3893–3899. [[CrossRef](#)]
100. Li, X.; Tong, T.; Wu, Q.; Guo, S.; Song, Q.; Han, J.; Huang, Z. Unique Seamlessly Bonded CNT@Graphene Hybrid Nanostructure Introduced in an Interlayer for Efficient and Stable Perovskite Solar Cells. *Adv. Funct. Mater.* **2018**, *28*, 1800475. [[CrossRef](#)]
101. Kladaew, M.; Lin, J.-Y.; Chanlek, N.; Vailikhit, V.; Hasin, P. Well-Dispersive Polypyrrole and MoSe<sub>2</sub> Embedded in Multiwalled Carbon Nanotube@Reduced Graphene Oxide Nanoribbon Electrocatalysts as the Efficient Counter Electrodes in Rigid and Plastic Dye-Sensitized Solar Cells. *ACS Appl. Energy Mater.* **2022**. [[CrossRef](#)]
102. Mohammed, K.A.; Alebadi, S.N.; Ziadan, K.; Al-kabbi, A.S.; Alrubaie, A.J.; Hussein, H.M. Organic-inorganic hybrid material: Synthesis, characterization for solar cell application. *J. Ovonic Res.* **2022**, *18*, 75–82. [[CrossRef](#)]
103. Liu, R. Hybrid Organic/Inorganic Nanocomposites for Photovoltaic Cells. *Materials* **2014**, *7*, 2747–2771. [[CrossRef](#)] [[PubMed](#)]
104. Tala-Ighil, R. Nanomaterials in Solar Cells. In *Handbook of Nanoelectrochemistry*; Aliofkhaezraei, M., Makhlof, A., Eds.; Springer: Cham, Switzerland, 2015; pp. 1–18.
105. Wu, Y.; Wu, X.; Guan, Y.; Xu, Y.; Shi, F.; Liang, J. Carbon-based flexible electrodes for electrochemical potassium storage. *New Carbon Mater.* **2022**, *37*, 852–874. [[CrossRef](#)]
106. Khanna, V.K. *Nano-Structured Photovoltaics: Solar Cells in the Nanotechnology Era*; CRC Press: Boca Rton, FL, USA, 2022.
107. IRENA; IEA-PVPS. *End-of-Life Management: Solar Photovoltaic Panels*; International Renewable Energy Agency (IRENA): Bonn, Germany; International Energy Agency Photovoltaic Power Systems Programme (IEA-PVPS): Washington, DC, USA, 2016.

108. Cheng, T.-H.; Liu, C.-J.; Tsai, T.-Y.; Shen, Y.-H. A Process for the Recovery of Gallium from Gallium Arsenide Scrap. *Processes* **2019**, *7*, 921. [\[CrossRef\]](#)
109. Walzberg, J.; Carpenter, A.; Heath, G.A. Role of the social factors in success of solar photovoltaic reuse and recycle programmes. *Nat. Energy* **2021**, *6*, 913–924. [\[CrossRef\]](#)
110. Zhang, X.; Xu, W.; Wang, S.; Liu, D.; Deng, P.; Deng, J.; Jiang, W. Research Status of Recovery of Tellurium from Cadmium Telluride Photovoltaic Modules. *IOP Conf. Ser. Mater. Sci. Eng.* **2020**, *782*, 022024. [\[CrossRef\]](#)
111. Liu, F.-W.; Cheng, T.-M.; Chen, Y.-J.; Yueh, K.-C.; Tang, S.-Y.; Wang, K.; Wu, C.-L.; Tsai, H.-S.; Yu, Y.-J.; Lai, C.-H.; et al. High-yield recycling and recovery of copper, indium, and gallium from waste copper indium gallium selenide thin-film solar panels. *Sol. Energy Mater. Sol. Cells* **2022**, *241*, 111691. [\[CrossRef\]](#)
112. Sharma, R.; Gupta, A.; Nandan, G.; Dwivedi, G.; Kumar, S. Life span and overall performance enhancement of Solar Photovoltaic cell using water as coolant: A recent review. *Mater. Today Proc.* **2018**, *5*, 18202–18210. [\[CrossRef\]](#)
113. Smith, S.E.; Stanislawski, B.J.; Eng, B.K.; Ali, N.; Silverman, T.J.; Calaf, M.; Cal, R.B. Viewing convection as a solar farm phenomenon broadens modern power predictions for solar photovoltaics. *J. Renew. Sustain. Energy* **2022**, *14*, 063502. [\[CrossRef\]](#)
114. Muchuweni, E.; Mombeshora, E.T.; Martincigh, B.S.; Nyamori, V.O. Recent Applications of Carbon Nanotubes in Organic Solar Cells. *Front. Chem.* **2021**, *9*, 733552. [\[CrossRef\]](#)
115. Khan, D.; Ali, Z.; Asif, D.; Kumar-Panjwani, M.; Khan, I. Incorporation of carbon nanotubes in photoactive layer of organic solar cells. *Ain Shams Eng. J.* **2021**, *12*, 897–900. [\[CrossRef\]](#)
116. Jagadeesh, K.; Chengaiah, C. A comprehensive review—Partial shading issues in PV system. *AIP Conf. Proc.* **2022**, *2640*, 020030. [\[CrossRef\]](#)
117. Aicha, D.; Bessous, N.; Rezaoui, M.M.; Merzouk, I. Study of the Effects of Partial Shading on PV Array. In Proceedings of the 2018 International Conference on Communications and Electrical Engineering (ICCEE), El Oued, Algeria, 17–18 December 2018.
118. Teo, J.C.; Tan, R.H.G.; Mok, V.H.; Ramachandaramurthy, V.K.; Tan, C. Impact of Partial Shading on the P-V Characteristics and the Maximum Power of a Photovoltaic String. *Energies* **2018**, *11*, 1860. [\[CrossRef\]](#)
119. Pendem, S.R.; Mikkili, S. Modeling, simulation, and performance analysis of PV array configurations (Series, Series-Parallel, Bridge-Linked, and Honey-Comb) to harvest maximum power under various Partial Shading Conditions. *Int. J. Green Energy* **2018**, *15*, 795–812. [\[CrossRef\]](#)
120. Bonthagorla, P.K.; Mikkili, S. Performance analysis of PV array configurations (SP, BL, HC and TT) to enhance maximum power under non-uniform shading conditions. *Eng. Rep.* **2020**, *2*, e12214. [\[CrossRef\]](#)
121. Tey, K.S.; Mekhilef, S.; Member, S.; Seyedmahmoudian, M. Improved Differential Evolution-based MPPT Algorithm using SEPIC for PV Systems under Partial Shading Conditions and Load Variation. *IEEE Trans. Ind. Inform.* **2018**, *14*, 4322–4333. [\[CrossRef\]](#)
122. Kabra, D.; Agarwal, V. A Review on: IoT based solar charge controller. *Int. J. Mech. Eng.* **2022**, *7*, 24–29.
123. Joshi, A.S.; Dincer, I.; Reddy, B.V. Performance analysis of photovoltaic systems: A review. *Renew. Sustain. Energy Rev.* **2009**, *13*, 1884–1897. [\[CrossRef\]](#)
124. Kamran, M.; Mudassar, M.; Fazal, M.R.; Asghar, M.U.; Bilal, M.; Asghar, R. Implementation of improved Perturb & Observe MPPT technique with confined search space for standalone photovoltaic system. *J. King Saud Univ. Eng. Sci.* **2020**, *32*, 432–441. [\[CrossRef\]](#)
125. Shang, L.; Guo, H.; Zhu, W. An improved MPPT control strategy based on incremental conductance algorithm. *Prot. Control Mod. Power Syst.* **2020**, *5*, 14. [\[CrossRef\]](#)
126. Ricco, M.; Hammami, M.; Mandrioli, R.; Grandi, G. Ripple Correlation Control MPPT Scheme Applied to a Three-Phase Flying Capacitor PV System. In *ELECTRIMACS 2019*; Springer: Cham, Switzerland, 2020; Volume 697, pp. 13–24.
127. Chen, L.; Wang, X. Enhanced MPPT method based on ANN-assisted sequential Monte-Carlo and quickest change detection. *IET Smart Grid* **2019**, *2*, 635–644. [\[CrossRef\]](#)
128. Cui, Y.; Yi, Z.; Duan, J.; Shi, D.; Wang, Z. A Rprop-Neural-Network-Based PV Maximum Power Point Tracking Algorithm with Short-Circuit Current Limitation. In Proceedings of the 2019 IEEE Power & Energy Society Innovative Smart Grid Technologies Conference (ISGT), Washington, DC, USA, 18–21 February 2019; p. 18902561.
129. Abdulridha, H.M.; Shaker, M.; Jaafar, H.F. Tracking of Maximum Power Point for PV Solar System Based on Adaptive Quantum Neural Controller. *Int. J. Intell. Eng. Syst.* **2022**, *15*, 382–396. [\[CrossRef\]](#)
130. Aly, M.; Rezk, H. An improved fuzzy logic control-based MPPT method to enhance the performance of PEM fuel cell system. *Neural Comput. Appl.* **2022**, *34*, 4555–4566. [\[CrossRef\]](#)
131. Li, D.; Li, J.; Wang, N. A Novel Technique Based on Peafowl Optimization Algorithm for Maximum Power Point Tracking of PV Systems Under Partial Shading Condition. *Front. Energy Res.* **2021**, *9*, 801571. [\[CrossRef\]](#)
132. Mo, S.; Ye, Q.; Jiang, K.; Mo, X.; Shen, G. An improved MPPT method for photovoltaic systems based on mayfly optimization algorithm. *Energy Reports* **2022**, *8*, 141–150. [\[CrossRef\]](#)
133. Alanazi, A.; Alanazi, M.; Arabi, S.; Sarker, S. A New Maximum Power Point Tracking Framework for Photovoltaic Energy Systems Based on Remora Optimization Algorithm in Partial Shading Conditions. *Appl. Sci.* **2022**, *12*, 3828. [\[CrossRef\]](#)
134. Eltamaly, A.M. An Improved Cuckoo Search Algorithm for Maximum Power Point Tracking of Photovoltaic Systems under Partial Shading Conditions. *Energies* **2021**, *14*, 953. [\[CrossRef\]](#)
135. Tan, W.-H.; Mohamad-Saleh, J. Modified normative fish swarm algorithm for optimizing power extraction in photovoltaic systems. *Evol. Intell.* **2022**, *1*–20. [\[CrossRef\]](#)

136. Subramaniana, A.; Ramanb, J. Modified Seagull Optimization Algorithm based MPPT for augmented performance of Photovoltaic solar energy systems. *Automatika* **2022**, *63*, 1–15. [[CrossRef](#)]
137. Chao, K.-H.; Rizal, M.N. A Hybrid MPPT Controller Based on the Genetic Algorithm and Ant Colony Optimization for Photovoltaic Systems under Partially Shaded Conditions. *Energies* **2021**, *14*, 2902. [[CrossRef](#)]
138. Dagal, I.; Akin, B.; Akboy, E. MPPT mechanism based on novel hybrid particle swarm optimization and salp swarm optimization algorithm for battery charging through simulink. *Sci. Rep.* **2022**, *12*, 2664. [[CrossRef](#)]
139. Padmanaban, S.; Priyadarshi, N.; Bhaskar, M.S.; Holm-Nielsen, J.B.; Ramachandaramurthy, V.K.; Hossain, E. A Hybrid ANFIS-ABC Based MPPT Controller for PV System With Anti-Islanding Grid Protection: Experimental Realization. *IEEE Access* **2019**, *7*, 103377–103389. [[CrossRef](#)]
140. Rahman, M.M.; Islam, M.S. PSO and ANN Based Hybrid MPPT Algorithm for Photovoltaic Array under Partial Shading Condition. *Eng. Int.* **2020**, *8*, 9–24. [[CrossRef](#)]
141. Priyadarshi, N.; Padmanaban, S.; Holm-Nielsen, J.B.; Blaabjerg, F.; Bhaskar, M.S. An Experimental Estimation of Hybrid ANFIS-PSO-Based MPPT for PV Grid Integration Under Fluctuating Sun Irradiance. *IEEE Syst. J.* **2020**, *14*, 1218–1229. [[CrossRef](#)]
142. Ali, M.N.; Mahmoud, K.; Lehtonen, M.; Darwish, M.M.F. Promising MPPT Methods Combining Metaheuristic, Fuzzy-Logic and ANN Techniques for Grid-Connected Photovoltaic. *Sensors* **2021**, *21*, 1244. [[CrossRef](#)] [[PubMed](#)]
143. Farzaneh, J. A hybrid modified FA-ANFIS-P&O approach for MPPT in photovoltaic systems under PSCs. *Int. J. Electron.* **2020**, *107*, 703–718. [[CrossRef](#)]
144. Panimalar, S.A. Nature Inspired Metaheuristic Algorithms. *Int. Res. J. Eng. Technol.* **2017**, *4*, 306–309.
145. Abdollahzadeh, B.; Gharehchopogh, F.S.; Khodadadi, N.; Mirjalili, S. Mountain Gazelle Optimizer: A new Nature-inspired Metaheuristic Algorithm for Global Optimization Problems. *Adv. Eng. Softw.* **2022**, *174*, 103282. [[CrossRef](#)]
146. Wang, L.; Cao, Q.; Zhang, Z.; Mirjalili, S.; Zhao, W. Artificial rabbits optimization: A new bio-inspired meta-heuristic algorithm for solving engineering optimization problems. *Eng. Appl. Artif. Intell.* **2022**, *114*, 105082. [[CrossRef](#)]
147. Zhao, S.; Zhang, T.; Ma, S.; Chen, M. Dandelion Optimizer: A nature-inspired metaheuristic algorithm for engineering applications. *Eng. Appl. Artif. Intell.* **2022**, *114*, 105075. [[CrossRef](#)]
148. Agushakaa, J.O.; Ezugwua, A.E.; Abualigah, L. Dwarf Mongoose Optimization Algorithm. *Comput. Methods Appl. Mech. Eng.* **2022**, *391*, 114570. [[CrossRef](#)]
149. Trojovský, P.; Deghani, M. Pelican Optimization Algorithm: A Novel Nature-Inspired Algorithm for Engineering Applications. *Sensors* **2022**, *22*, 855. [[CrossRef](#)] [[PubMed](#)]
150. Peraza-Vázquez, H.; Peña-Delgado, A.F.; Echavarría-Castillo, G.; Morales-Cepeda, A.B.; Velasco-Álvarez, J.; Ruiz-Perez, F. A Bio-Inspired Method for Engineering Design Optimization Inspired by Dingoes Hunting Strategies. *Math. Probl. Eng.* **2021**, *2021*, 9107547. [[CrossRef](#)]
151. Abdollahzadeh, B.; Gharehchopogh, F.S.; Mirjalili, S. African vultures optimization algorithm: A new nature-inspired metaheuristic algorithm for global optimization problems. *Comput. Ind. Eng.* **2021**, *158*, 107408. [[CrossRef](#)]
152. Hayyolalam, V.; Kazem, A.A.P. Black Widow Optimization Algorithm: A novel meta-heuristic approach for solving engineering optimization problems. *Eng. Appl. Artif. Intell.* **2020**, *87*, 103249. [[CrossRef](#)]
153. Zervoudakis, K.; Tsafarakis, S. A mayfly optimization algorithm. *Comput. Ind. Eng.* **2020**, *145*, 106559. [[CrossRef](#)]
154. Harifi, S.; Khalilian, M.; Mohammadzadeh, J.; Ebrahimnejad, S. Emperor Penguins Colony: A new metaheuristic algorithm for optimization. *Evol. Intell.* **2019**, *12*, 211–226. [[CrossRef](#)]
155. Heidari, A.A.; Mirjalili, S.; Faris, H.; Aljarah, I.; Mafarja, M.; Chen, H. Harris hawks optimization: Algorithm and applications. *Futur. Gener. Comput. Syst.* **2019**, *97*, 849–872. [[CrossRef](#)]
156. Kaveh, A.; Kooshkebaghi, M. Artificial coronary circulation system: A new bio-inspired metaheuristic algorithm. *Sci. Iran. Int. J. Sci. Technol.* **2019**, *26*, 2731–2747. [[CrossRef](#)]
157. Mahmood, M.; Al-Khateeb, B. The blue monkey: A new nature inspired metaheuristic optimization algorithm. *Period. Eng. Nat. Sci.* **2019**, *7*, 1054–1066. [[CrossRef](#)]
158. Gomes, G.F.; Cunha, S.S.; Ancelotti, A. A sunflower optimization (SFO) algorithm applied to damage identification on laminated composite plates. *Eng. Comput.* **2019**, *35*, 619–626. [[CrossRef](#)]
159. Mhawesh, M.A.; Neda, O.M. A Review of the Photovoltaic System Converters and Algorithms. *J. Glob. Sci. Res.* **2021**, *6*, 1297–1308.
160. Baharudin, N.H.; Mansur, T.M.N.T.; Hamid, F.A.; Ali, R.; Irwanto, M. Topologies of DC-DC Converter in Solar PV Applications. *Indones. J. Electr. Eng. Comput. Sci.* **2017**, *8*, 368–374. [[CrossRef](#)]
161. Sutikno, T.; Purnama, H.S.; Widodo, N.S.; Padmanaban, S.; Sahid, M.R. A review on non-isolated low-power DC-DC converter topologies with high output gain for solar photovoltaic system applications. *Clean Energy* **2022**, *6*, 557–572. [[CrossRef](#)]
162. Sri-Revathi, B.; Prabhakar, M. Non isolated high gain DC-DC converter topologies for PV applications—A comprehensive review. *Renew. Sustain. Energy Rev.* **2016**, *66*, 920–933. [[CrossRef](#)]
163. Radhika, S.; Margaret, V. A Review on DC-DC Converters with Photovoltaic System in DC Micro Grid. *J. Phys. Conf. Ser.* **2021**, *1804*, 012155. [[CrossRef](#)]
164. Kiran, S.U.; Kumar, P.M.; Kumar, Y.V.P. Comprehensive Analysis on Critical Factors for the Operation of Advanced High Gain DC-DC Converters Used in Renewable Energy Applications. *Int. J. Renew. Energy Res.* **2021**, *11*, 1448–1459.
165. Sarangi, S.; Verma, H.K. Step up DC-DC converters for PV applications: A Review. *J. Controll. Convert.* **2018**, *3*, 1–7.

166. Erdiwansyah; Mahidin; Husin, H.; Nasaruddin; Zaki, M.; Muhibbuddin. A critical review of the integration of renewable energy sources with various technologies. *Prot. Control Mod. Power Syst.* **2021**, *6*, 3. [CrossRef]
167. Sivakumar, S.; Sathik, M.J.; Manoj, P.S.; Sundararajan, G. An assessment on performance of DC–DC converters for renewable energy applications. *Renew. Sustain. Energy Rev.* **2016**, *58*, 1475–1485. [CrossRef]
168. Babaa, S.E.; El Murr, G.; Mohamed, F.; Pamuri, S. Overview of Boost Converters for Photovoltaic Systems. *J. Power Energy Eng.* **2018**, *6*, 16–31. [CrossRef]
169. Fulmali, V.; Gupta, S.; Khan, M.F. Modeling and simulation of boost converter for solar-PV energy system to enhance its output. In Proceedings of the 2015 International Conference on Computer, Communication and Control (IC4), Indore, India, 10–12 September 2015; p. 15700301.
170. Srikanth, M.; Upadhyay, P.; Kalyani, S.T. Design and Development of Buck/Boost Converter for Maintaining the Constant DC Supply to Meet the Load Requirement. *Int. J. Eng. Technol.* **2018**, *7*, 215–220. [CrossRef]
171. Supraptono, E.; Abiyasa, B.P.; Putri, R.D.M.; Andrasto, T. The effect of the performance of using a boost converter on the voltage of the solar panel. *IOP Conf. Ser. Earth Environ. Sci.* **2022**, *969*, 012028. [CrossRef]
172. Pauldoss, S.P.; Sekar, K.; Pattanaik, B.; Nayagam, V.S. PV system with high voltage gain based DC-DC boost converter for grid applications. *AIP Conf. Proc.* **2022**, *2519*, 050007. [CrossRef]
173. Chandramouli, A.; Sivachiadambaranathan, V. Design and Analysis of a Photovoltaic System with a DC-DC Boost Converter. In Proceedings of the 2019 3rd International Conference on Computing Methodologies and Communication (ICCMC, Erode, India, 27–29 March 2019; p. 18958390.
174. Mohamed, H.A.; Khattab, H.A.; Mobarka, A.; Morsy, G.A. Design, control and performance analysis of DC-DC boost converter for stand-alone PV system. In Proceedings of the 2016 Eighteenth International Middle East Power Systems Conference (MEPCON, Cairo, Egypt, 27–29 December 2016; p. 16640325.
175. Omar, M.A.; Mahmoud, M.M. Design and Simulation of DC/DC Boost Converter with Maximum Power Point Tracking for Grid Connected PV Inverter Considering the Nonlinearity of the PV Generator. *Int. J. Energy Convers.* **2019**, *7*, 241–252. [CrossRef]
176. Raj, A.; Praveen, R.P. Highly efficient DC-DC boost converter implemented with improved MPPT algorithm for utility level photovoltaic applications. *Ain Shams Eng. J.* **2022**, *13*, 101617. [CrossRef]
177. Hashim, N.; Salam, Z.; Johari, D.; Ismail, N.F.N. DC-DC Boost Converter Design for Fast and Accurate MPPT Algorithms in Stand-Alone Photovoltaic System. *Int. J. Power Electron. Drive Syst.* **2018**, *9*, 1038–1050. [CrossRef]
178. Saravanan, S.; Babu, N.R. A modified high step-up non-isolated DC-DC converter for PV application. *J. Appl. Res. Technol.* **2017**, *15*, 242–249. [CrossRef]
179. Veerabhadra; Rao, S.N. Assessment of high-gain quadratic boost converter with hybrid-based maximum power point tracking technique for solar photovoltaic systems. *Clean Energy* **2022**, *6*, 632–645. [CrossRef]
180. Esfahani, F.N.; Darwish, A.; Williams, B.W. Power Converter Topologies for Grid-Tied Solar Photovoltaic (PV) Powered Electric Vehicles (EVs)—A Comprehensive Review. *Energies* **2022**, *15*, 4648. [CrossRef]
181. Supriya, J.; Rajashekar, J.S. A Comprehensive Review of Various Isolated DC-DC Converters Topologies Associated with Photovoltaic Applications. *Recent Adv. Electr. Electron. Eng. (Former. Recent Pat. Electr. Electron. Eng.)* **2022**, *15*, 595–606. [CrossRef]
182. Reshma-Gopi, R.; Sreejith, S. Converter topologies in photovoltaic applications—A review. *Renew. Sustain. Energy Rev.* **2018**, *94*, 1–14. [CrossRef]
183. Salehi, N.; Martínez-García, H.; Velasco-Quesada, G. Modified Cascaded Z-Source High Step-Up Boost Converter. *Electronics* **2020**, *9*, 1932. [CrossRef]
184. Dahono, P.A. Simplified cascade multiphase DC-DC boost power converters for high voltage-gain and low-ripple applications. *Int. J. Power Electron. Drive Syst.* **2021**, *12*, 273–285. [CrossRef]
185. Krishnaveni, S.; Rajini, V.; Krishnaveni, S.; Rajini, V. Cascaded boost converter-based high-voltage pulse generator for pulsed electric field applications. *Arch. Electr. Eng.* **2021**, *70*, 631–641. [CrossRef]
186. Pal, N.; Fish, A.; McIntyre, W.; Griesert, N.; Winter, G.; Eichhorn, T.; Pilawa-Podgurski, R.; Hanumolu, P.K. A 91.15% Efficient 2.3–5-V Input 10–35-V Output Hybrid Boost Converter for LED-Driver Applications. *IEEE J. Solid-State Circuits* **2021**, *56*, 3499–3510. [CrossRef]
187. Kumari, R.; Pyakurel, P.; Rai, B.; Pandit, M.; Sherpa, K.S.; Bhattacharya, D. Design of Smart Autonomous Solar Panel with Cascaded Sepic-Boost Converter for High Voltage Renewable Applications. 2022, pp. 1–18. Available online: <https://www.researchsquare.com/article/rs-1880316/v1> (accessed on 18 December 2022).
188. Zhang, H.; Park, S.-J. Efficiency Optimization Method for Cascaded Two-Stage Boost Converter. *IEEE Access* **2022**, *10*, 53443–53453. [CrossRef]
189. Alghaythi, M.L.; O’Connell, R.M.; Islam, N.E.; Khan, M.M.S.; Guerrero, J.M. A High Step-Up Interleaved DC-DC Converter With Voltage Multiplier and Coupled Inductors for Renewable Energy Systems. *IEEE Access* **2020**, *8*, 2169–3536. [CrossRef]
190. Yaseen, M.; Farooq, A.; Malik, M.Z.; Usman, M.; Hafeez, G.; Ali, M. Design of a High Step-Up DC-DC Converter with Voltage Doubler and Tripler Circuits for Photovoltaic Systems. *Int. J. Photoenergy* **2021**, *2021*, 8993598. [CrossRef]
191. Rahimi, T.; Ding, L.; Gholizadeh, H.; Shahrivar, R.S.; Faraji, R. An Ultra High Step-Up DC–DC Converter Based on the Boost, Luo, and Voltage Doubler Structure: Mathematical Expression, Simulation, and Experimental. *IEEE Access* **2021**, *9*, 132011–132024. [CrossRef]

192. Jarin, T.; Akkara, S.; Mole, S.S.S.; Manivannan, A.; Immanuel-Selvakumar, A. Fuel vehicle improvement using high voltage gain in DC-DC boost converter. *Renew. Energy Focus* **2022**, *43*, 228–238. [[CrossRef](#)]
193. Alkhalidi, A.; Akbar, F.; Elkhateb, A.; Laverty, D. N-stage quadratic boost converter based on voltage lift technique and voltage multiplier. In Proceedings of the 11th International Conference on Power Electronics, Machines and Drives (PEMD 2022), IET, Hybrid Conference, Newcastle, UK, 21–23 June 2022.
194. Mohseni, P.; Mohammadsalehian, S.; Islam, M.R.; Muttaqi, K.M.; Sutanto, D.; Alavi, P. Ultrahigh Voltage Gain DC–DC Boost Converter With ZVS Switching Realization and Coupled Inductor Extendable Voltage Multiplier Cell Techniques. *IEEE Trans. Ind. Electron.* **2022**, *69*, 323–335. [[CrossRef](#)]
195. Rashmi, R.; Kumar, T.S. DC Booster with Voltage Multiplier for Renewable Energy Sources. *J. Res. Appl. Sci. Eng. Technol.* **2022**, *10*, 2460–2466. [[CrossRef](#)]
196. Rosas, I.P.; Agostini, E.; Nascimento, C.B. Single-Switch High-Step-Up DC-DC Converter Employing Coupled Inductor and Voltage Multiplier Cell. *IEEE Access* **2022**, *10*, 82626–82635. [[CrossRef](#)]
197. Photong, C.; Piansangsan, L. High Efficiency High Voltage Gain Boost Converter using Zero Crossing Switching Multi-stage Voltage-Lift Cells. *Prz. Elektrotechniczny* **2020**, *1*, 71–75. [[CrossRef](#)]
198. Khan, S.; Mahmood, A.; Zaid, M.; Tariq, M.; Lin, C.-H.; Ahmad, J.; Alamri, B.; Alahmadi, A. A High Step-up DC-DC Converter Based on the Voltage Lift Technique for Renewable Energy Applications. *Sustainability* **2021**, *13*, 11059. [[CrossRef](#)]
199. Jana, A.S.; Lin, C.-H.; Kao, T.-H.; Chang, C.-H. A High Gain Modified Quadratic Boost DC-DC Converter with Voltage Stress Half of Output Voltage. *Appl. Sci.* **2022**, *12*, 4914. [[CrossRef](#)]
200. Khan, S.; Zaid, M.; Siddique, M.D.; Iqbal, A. Ultra high gain step up DC/DC converter based on switched inductor and improved voltage lift technique for high-voltage applications. *IET Power Electron.* **2022**, *15*, 1–21. [[CrossRef](#)]
201. Fares, O.S.; Hussien, J.F. High gain multiphase boost converter based-on capacitor clamping structure. *Indones. J. Electr. Eng. Comput. Sci.* **2021**, *24*, 689–696. [[CrossRef](#)]
202. Alsolami, M. A multi-input, multi-stage step-up DC-DC converter for PV applications. *Alexandria Eng. J.* **2021**, *60*, 2315–2324. [[CrossRef](#)]
203. Saravanakumar, T.; Kumar, R.S. Design, Validation, and Economic Behavior of a Three-Phase Interleaved Step-Up DC–DC Converter for Electric Vehicle Application. *Front. Energy Res.* **2022**, *10*, 813081. [[CrossRef](#)]
204. Sampath, S.; Rahiman, Z.; Chenniappan, S.; Sundaram, E.; Subramaniam, U.; Padmanaban, S. Efficient Multi-Phase Converter for E-Mobility. *World Electr. Veh. J.* **2022**, *13*, 67. [[CrossRef](#)]
205. Billy, I.J.; Hussein, J.F. Non-isolated high voltage gain DC to DC converter based on the diode a capacitor switches. *Indones. J. Electr. Eng. Comput. Sci.* **2022**, *28*, 67–75. [[CrossRef](#)]
206. Hu, D.; Yin, A.; Ghaderi, D. A transformer-less single-switch boost converter with high-voltage gain and mitigated-voltage stress applicable for photovoltaic utilizations. *Int. Trans. Electr. Energy Syst.* **2020**, *30*, e12569. [[CrossRef](#)]
207. Abdel-Rahim, O.; Abdelhameed, E.H. Ultimate Transformerless Boost DC-DC Converter for Renewable Energy Applications. *SVU-Int. J. Eng. Sci. Appl.* **2021**, *2*, 63–69. [[CrossRef](#)]
208. Sadaf, S.; Bhaskar, M.S.; Meraj, M.; Iqbal, A.; Al-Emadi, N. Transformer-Less Boost Converter With Reduced Voltage Stress for High Voltage Step-Up Applications. *IEEE Trans. Ind. Electron.* **2021**, *69*, 1498–1508. [[CrossRef](#)]
209. Babaei, E.; Maheri, H.M.; Sabahi, M. A transformer-less DC–DC converter with high voltage conversion ratio adopting inverting voltage lift cell. *IET Circuits Devices Syst.* **2021**, *16*, 257–271. [[CrossRef](#)]
210. Zhao, J.; Chen, D.; Jiang, J. Transformerless High Step-Up DC-DC Converter with Low Voltage Stress for Fuel Cells. *IEEE Access* **2021**, *9*, 10228–10238. [[CrossRef](#)]
211. Saravanan, S.; Rani, P.U.; Thakre, M.P. Evaluation and Improvement of a Transformerless High-Efficiency DC–DC Converter for Renewable Energy Applications Employing a Fuzzy Logic Controller. *MAPAN—J. Metrol. Soc. India* **2022**, *37*, 291–310. [[CrossRef](#)]
212. Ahmed, H.Y.; Abdel-Rahim, O.; Ali, Z.M. New High-Gain Transformerless DC/DC Boost Converter System. *Electronics* **2022**, *11*, 734. [[CrossRef](#)]
213. Revathi, B.S.; Mahalingam, P. Non-isolated high gain DC–DC converter with low device stress and input current ripple. *IET Power Electron.* **2018**, *11*, 2553–2562. [[CrossRef](#)]
214. Zhang, N.; Sutanto, D.; Muttaqi, K.M. A review of topologies of three-port DC–DC converters for the integration of renewable energy and energy storage system. *Renew. Sustain. Energy Rev.* **2016**, *56*, 388–401. [[CrossRef](#)]

**Disclaimer/Publisher’s Note:** The statements, opinions and data contained in all publications are solely those of the individual author(s) and contributor(s) and not of MDPI and/or the editor(s). MDPI and/or the editor(s) disclaim responsibility for any injury to people or property resulting from any ideas, methods, instructions or products referred to in the content.